Coordination Chemistry Reviews, 88 (1988) 1–68
Elsevier Science Publishers B.V., Amsterdam – Printed in The Netherlands

STRUCTURE AND PROPERTIES OF METALLOPORPHYRINS AND HEMOPROTEINS: THE VIBRONIC APPROACH

I.B. BERSUKER and S.S. STAVROV

Institute of Chemistry, Academy of Sciences, Moldavian SSR, Kishinev 277028 (U.S.S.R.)

(Received 28 May 1987)

CONTENTS

A. Introduction . . . 2
B. The concept of vibronic interactions in stereochemical and electron–conformational problems . . . 3
C. Vibronic origin of the metal position and spin state of four-coordinate metalloporphyrins . . . 8
  (i) Adiabatic potentials for different electronic states . . . 10
  (ii) Ground state multiplicity and geometry . . . 14
D. Stereochemistry of metalloporphyrin and hemoprotein active centre complexes with axial ligands . . . 18
  (i) Perturbation theory for geometry changes by coordination . . . 18
  (ii) Application to the spin state/metal position relationship . . . 21
  (iii) Geometries of coordination of diatomics . . . 29
E. Photolysis of complexes with diatomics . . . 37
  (i) Formulation of the problem . . . 38
  (ii) Influence of vibronic effects on the magnitude of the activation barrier to photodecay . . . 41
  (iii) Mechanism of photolysis . . . 45
  (iv) Discussion of results . . . 47
F. Vibronic effects in excited *B* and *Q* states . . . 49
  (i) The four-orbital model . . . 49
  (ii) Vibronic effect manifestations . . . 51
  (iii) Simultaneous effect of vibronic interactions and low symmetry external fields . . . 53
  (iv) Splitting of the *B* and *Q* absorption bands . . . 55
G. Concluding remarks . . . 58
References . . . 59

ABBREVIATIONS

Porphyrins

(EtioP)	etioporphyrin
(OEP)	octaethylporphyrin
(P)	any porphyrin

0010-8545/88/$10.85

(Por)	porphine
(TBP)	tetrabenzporphyrin
(TPP)	tetraphenylporphyrin
(Pc)	phthalocyanine

Hemoproteins

Hb	hemoglobin
HP	any hemoprotein
Mb	myoglobin

Ligands

Im	imidazole
1-MeIm	1-methylimidazole
2-MeIm	2-methylimidazole
py	pyridine

A. INTRODUCTION

The well-known class of hemoproteins (HP) with metalloporphyrins (Me(P)) as active centres performs a wide range spectrum of functions from oxygen transport by hemoglobin to hydroxylation of saturated hydrocarbons by cytochrome P-450. Much effort has been devoted to the study of the properties of these systems using all possible physical methods of investigation. In these investigations special attention is paid to the geometry and electronic structure of these systems especially of their active centres, which are directly coupled to almost all the physical observables. For many years, the study of the electronic structure of molecular systems was limited mainly to the determination of electronic energy levels and wavefunctions (molecular orbitals (MO)) for fixed nuclei, information that answered many questions concerning the structure and mechanisms of the functioning of these systems.

During the last quarter of this century, the theory of molecular structure (including electronic structure) was extended through the vibronic approach. The main goal of this approach is better understanding of the influence of electrons on nuclear configuration and dynamics (and vice versa) by means of an improvement on the full separation of electronic and nuclear motions in the crude adiabatic approximation. In its simple formulation this can be done by taking account of the mixing of the electronic states (obtained for fixed nuclei and fixed molecular geometry) under nuclear displacements. This approach reveals the origin of the stable molecular configurations, conditions of instability and the influence of electronic structure on nuclear configuration and its transformations, as well as all the consequent effects on observable properties.

The vibronic approach is widely used in all areas of the physics and chemistry of molecules and crystals [1–8]. In the applications to metalloporphyrins and hemoproteins reviewed in this paper, the vibronic approach elucidates a series of new qualitative and semiquantitative regularities in their properties and mechanisms of functioning. We have tried to take into consideration all the literature data on the problem, to make appropriate comparisons, and to note other points of view and approaches.

B. THE CONCEPT OF VIBRONIC INTERACTIONS IN STEREOCHEMICAL AND ELECTRON–CONFORMATIONAL PROBLEMS

The concept of vibronic interactions starts with the idea that in many problems of modern chemistry and physics the full separation of electronic and nuclear motions in the framework of the adiabatic approximation (AA) is invalid. It ignores many details of the electronic structure when analysing the nuclear configuration and its dynamics [1]. However, a complete rejection of the AA is neither necessary nor possible, since without this approximation the notion of molecular spatial configuration loses its meaning. A simple way to go beyond the AA is to start with electronic states for fixed nuclei (crude AA) and then to take into account the mixing of these electronic states by nuclear displacements from the starting nuclear configuration (by the vibronic interaction terms in the Hamiltonian). This vibronic approach proved to be very efficient in molecular problems and revealed a series of new effects and regularities in all ranges of spectroscopy, stereochemistry and crystal chemistry and physics, including phase transitions, impurity crystal physics, chemical reactivity and activation [1–8].

The main idea of the vibronic approach may be illustrated by considering a simple example of a molecular system with two energy levels, ground and excited, which allows us also to introduce the notations used below (for details see ref. 1). Let us divide the Hamiltonian of the system H into three parts, $H = H_r + H_q + V(r, q)$, where H_r is the pure electronic part, H_q is the nuclear kinetic energy and $V(r, q)$ includes all the electron–nuclear and nuclear–nuclear interactions, r and q being the sets of electronic and symmetrized (normal) nuclear coordinates respectively. Let us expand $V(r, q)$ into a series with respect to small displacements of the nuclei from the initial high symmetry point $q = 0$ as follows:

$$V(r, q) = V(r, 0) + \sum_{\alpha} \left(\frac{\partial V}{\partial q_\alpha} \right)_0 q_\alpha + \frac{1}{2} \sum_{\alpha, \beta} \left(\frac{\partial^2 V}{\partial q_\alpha \partial q_\beta} \right)_0 q_\alpha q_\beta + \dots \tag{1}$$

and assume that by solving the Schrödinger equation with the zeroth order Hamiltonian $H' = H_r + V(r, 0)$ we obtained two non-degenerate states Ψ_1 and Ψ_2 (ground and excited) with energies E_1 and E_2. Then introducing the remaining terms of eqn. (1) (the vibronic interaction terms are not taken into account in the zeroth Hamiltonian H'), say, the first-order term in q, as a perturbation, we obtain the following secular equation for the dependence of the energy levels on q:

$$\begin{vmatrix} -\Delta - \mathscr{E}' & Fq \\ Fq & \Delta - \mathscr{E}' \end{vmatrix} = 0 \tag{2}$$

with roots $\mathscr{E}' = \pm(\Delta^2 + F^2q^2)^{1/2}$. Here

$$F = \left\langle \Psi_1 \middle| \left(\frac{\partial V}{\partial q} \right)_0 \middle| \Psi_2 \right\rangle \tag{3}$$

is the so-called vibronic constant determining the measure of mixing of the two states by nuclear displacements in the direction of the q coordinate. For non-zero F values, q has the symmetry of the product of symmetries of Ψ_1 and Ψ_2 (the energies are read off the middle of the interval $2\ \Delta = E_2 - E_1$). Taking account of the term $\frac{1}{2}K_0q^2$, where K_0 is the primary force constant (the average of the operator of quadratic vibronic interactions, see ref. 1), we obtain the following expressions for the electronic energy as a function of q (the adiabatic potential):

$$\mathscr{E}_1(q) = \frac{1}{2}K_0q^2 - (\Delta^2 + F^2q^2)^{1/2} = -\Delta + \frac{1}{2}\left(K_0 - \frac{F^2}{\Delta}\right)q^2 + \ldots$$

$$\mathscr{E}_2(q) + \frac{1}{2}K_0q^2 + (\Delta^2 + F^2q^2)^{1/2} = \Delta + \frac{1}{2}\left(K_0 + \frac{F^2}{\Delta}\right)q^2 - \ldots \tag{4}$$

Equation (4) shows that vibronic mixing lowers the force constant of the ground state from K_0 to $K_1 = K_0 - F^2/\Delta$ (this state is softened), while increasing that of the excited state to $K_2 = K_0 + F^2/\Delta$ (the state is hardened). If

$$F^2/\Delta \geqslant K_0 \tag{5}$$

the ground state becomes unstable with respect to small q displacements (Fig. 1).

The effect of instability or softening of the lower state owing to the vibronic mixing with the upper state is called the pseudo-Jahn–Teller effect [1] (distinguished from the Jahn–Teller effect when the two mixing states are degenerate at $q = 0$). The term "second-order Jahn–Teller effect" seems to be less acceptable since, as shown above, the effect occurs as an exact

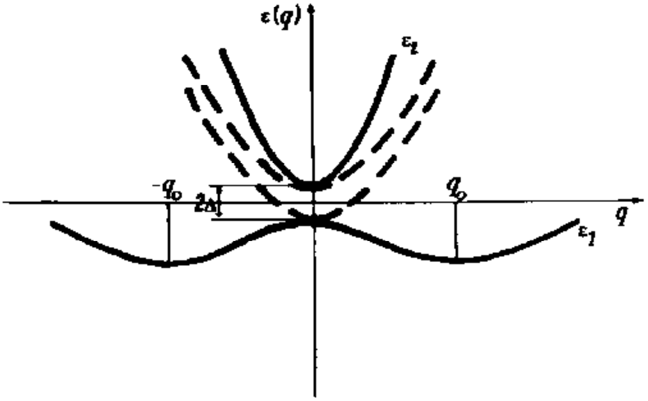

Fig. 1. The shape of the adiabatic potential sheets with (solid lines) and without (broken lines) the pseudo-Jahn–Teller effect for two non-degenerate mixing terms.

solution of a two-(many)-level problem (including all the orders of perturbation theory).

If there are several excited states, each of which mixes independently with the ground state under the q displacements, then for the force constant K we obtain

$$K = K_0 - \sum_i \frac{F_i^2}{\Delta_i} \tag{6}$$

where F_i is the vibronic constant of mixing with the ith state and $2\Delta_i$ is the energy distance to this state. In this case the vibronic instability occurs if

$$\sum_i F_i^2/\Delta_i \geqslant K_0 \tag{7}$$

The important question is the following. Is vibronic mixing of the ground electronic state with the excited states the only possible source of dynamic instability for polyatomic systems (negative K value), or can the non-vibronic part K_0 itself be negative? The answer is that in all cases when Coulomb forces are compensated, $K_0 \geqslant 0$, and hence instability in the q direction can occur due to (and only to) the vibronic mixing with excited states [9–11]. This statement was proved both in general (analytically) and for concrete systems by numerical ab initio calculations [10]. The latter also allows us to clarify the nature of the excited state causing the instability of the ground state and to obtain numerical estimates of all the contributions to the effect (all the parameters in eqn. (5) or (7)).

For a better understanding of the next sections we present here a visual interpretation of the pseudo-Jahn–Teller instability condition (eqn. (5)). What is the visual origin of the forces driving the system toward lower symmetry in the vibronic cases under consideration when the Coulomb

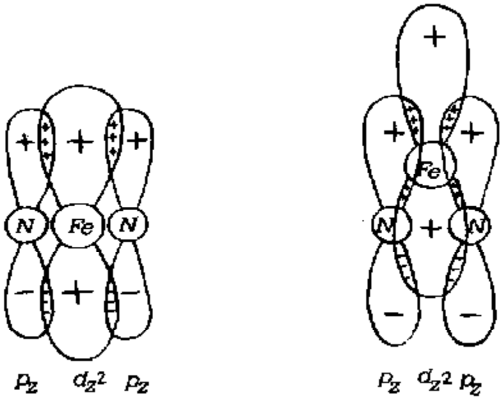

Fig. 2. Illustration of the visual treatment of the origin of the pseudo-Jahn–Teller effect using the N–Fe–N fragment of the square-planar FeN_4 molecular group as an example.

forces are compensated? To answer this question let us consider an example with a transition metal atom Me, having an unoccupied d_{z^2} orbital, surrounded by four nitrogen atoms with highest occupied $2p_z$ orbitals. The cross-section of this system along the line N–Me–N is shown schematically in Fig. 2. It is seen that when the Me atom lies in the plane of the four nitrogen atoms, the integral overlap of its d_{z^2} orbital with the nitrogen p_z orbitals equals zero, and hence no bonding between them is possible in this configuration. However, if the Me atom goes out of the plane of the nitrogen atoms, then the d_{z^2}–p_z integral overlap becomes non-zero, and additional Me–N π bonding occurs. The condition of eqn. (5) means that if the energy of this additional π bonding formed by the out-of-plane displacement of the Me atom is larger than that lost by the appropriate deterioration of the Me–N σ bonds, then this out-of-plane displacement of the Me atom is energetically favourable. Thus the forces driving the system toward lower symmetry in the pseudo-Jahn–Teller cases under consideration are nothing else than exchange forces of additional covalent bonds formed by this distortion.

In addition to this main contribution to the instability among the terms F_i^2/Δ_i in eqn. (5) or (7) there may also be terms originating from the mixing of orbitals of the same atom (either Fe or N in the above example). These terms have the physical meaning of electronic polarization due to distortion. As a rule the polarization contributions are an order of magnitude smaller than that of new covalencies. In the numerical results mentioned above [10], for instance, in the case of the NH_3 molecule, the nitrogen polarization term (the F_p^2/Δ_p value due to the $2p$–$3s$ mixing), which occurs owing to the nitrogen displacement out of the H_3 plane, equals $F_p^2/\Delta_p \approx 0.06$ mdyn Å^{-1}, whereas for the covalent contribution, $F_c^2/\Delta_c \approx 0.62$ mdyn Å^{-1}. Similar ratios between covalent and polarization contributions were obtained for systems with transition metals.

The condition for dynamic instability (eqn. (5)) is especially important for biological systems. Indeed, the latter possess many low frequency vibrations (soft modes) providing small K_0 values for appropriate nuclear displacements q. In combination with non-filled (open shell) close-in-energy d states of the active centres (small Δ values) the condition of instability (eqn. (5) or (7)) is most favourable. Having soft modes, the local distortion due to the vibronic instability moves easily along the system, resulting in conformational changes.

In biological systems such conformational transitions are usually initiated either by the appearance (disappearance, excitation) of one electron, or by a more complicated electronic rearrangement, for instance, caused by the coordination of another molecular system to the active centre [8] (electron-conformational transitions). In these cases the process can be more conveniently described by means of the so-called orbital vibronic constants $f_q^{(ij)}$ [1]. If we denote the changes in the MO occupation numbers by Δp_i, then the force F_q occurring as a result of this electronic rearrangement and acting upon the nuclear framework in the direction of the symmetrized displacements q equals [1,8]

$$F_q = \sum_i \Delta p_i f_q^i \tag{8}$$

where $f_q^i = f_{qq}^{(ii)}$ is the diagonal orbital vibronic constant having the meaning of the force with which the electron of the ith MO distorts the nuclear framework in the q direction (in the equilibrium state $F_q = \sum_i \Delta p_i f_q^i = 0$). With known orbital vibronic constants (some of them can be determined from spectroscopic data [1]) one can predict the direction and magnitude of the force F_q resulting from certain electron rearrangements, and the conformational transition caused by this force.

In application to stereochemical problems, the inequality (5) is a powerful means for the analysis of possible unstable (stable) molecular system configurations. Indeed, since the vibronic mixing is the only source of dynamic instability, then, starting with a certain (mostly high symmetry [1]) configuration of the nuclear framework, the inequality (5) can be employed to decide whether this configuration is stable. To do this one must know (at least approximately) the wavefunctions and energies of the electronic states which are mixed. The criterion of eqn. (5) is especially fruitful for comparisons of similar molecular systems. Many examples of this approach are in the literature [1,4,12].

In the present paper the concept of vibronic interactions in its widest meaning is used to analyse the structure (spatial configuration) and properties of metalloporphyrins and hemoproteins. Most attention is paid to the stereochemistry of metalloporphyrins and their complexes with different ligands, the origin of special features of photolysis, and optical absorption spectra. These observable properties, as shown below, are determined by the vibronic effects, in which the main contribution is due to the formation of new covalent bonding by distortion of the high symmetry configuration.

C. VIBRONIC ORIGIN OF THE METAL POSITION AND SPIN STATE OF FOUR-COORDINATE METALLOPORPHYRINS

The relationship between the nature of the metal and its position with respect to the porphyrin ring was the subject for long discussions (for reviews see refs. 13–17). In 1963, Hoard [18], generalizing the experimental data available at that time, put forward a hypothesis (which afterward developed into a concept [13,16]) that the internal radius of the porphyrin ring in the non-distorted and non-stressed state is 2.01 Å and the energy of its deformation is very high. Therefore the out-of-plane or in-plane position of the metal with respect to the porphyrin ring in the metal porphyrin is dependent on whether the sum of the radii of the metal and the pyrrole nitrogen is smaller or larger than the above magnitude. This approach attributes the out-of-plane position of the Fe(II) atom in high spin complexes (including deoxyhemoglobin) and its in-plane position in low spin complexes to the radius of the iron atom, which decreases when passing from the high spin to the low spin state. Indeed, the high spin state can be obtained from the low spin state by means of the excitation of one electron from the $d_{xz,yz}$ orbital to $b_{1g}(d_{x^2-y^2})$, resulting in an increase in the atomic dimensions in the xy plane (see Fig. 3).

Almost the same explanation for the out-of-plane position of the high spin iron atom was suggested by Perutz [19–23]. He assumed that in the high spin complexes the population of the $b_{1g}(d_{x^2-y^2})$ MO, which is antibonding with respect to the metal–porphyrin bond, results in a strong repulsion between the metal and the pyrrole nitrogen. This repulsion tends to increase the distance between them, the out-of-plane position of the iron atom being one of the possibilities to realize this increase in the interatomic distances. It should be noted that in both the Perutz and Hoard suggestions the possibility for ring deformation is completely ignored.

However, new experimental data contradict the Hoard–Perutz hypothesis. The X-ray analysis of Ag(P) and Zn(P) [24,25] shows that the metal occupies the in-plane position. This is in contradiction to the Hoard concept. Indeed, in these metals the $b_{1g}(d_{x^2-y^2})$ MO is populated, resulting in an ionic radius larger than that of the high spin iron atom [26]. Contrary to the Hoard concept, this leads not to an out-of-plane position of the metal, but to a

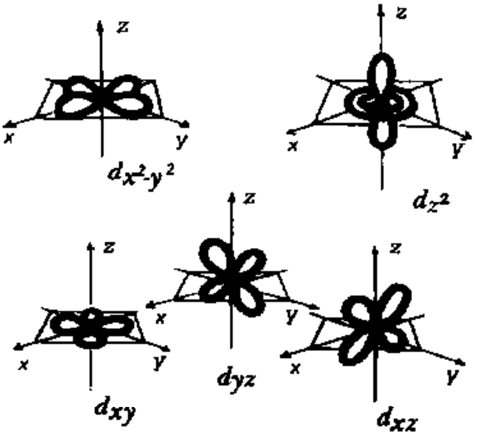

Fig. 3. Electron *d* orbital angular wavefunctions.

distortion (enlarging) of the cavity of the porphyrin ring (in Zn(P) its radius equals 2.04 Å [24,25], whereas in Ag(P) it is 2.09 Å [25]).

The same contradiction arises for phthalocyanine (Pc) complexes with different metals. Following the Hoard concept the optimal radius of the (Pc) cavity is 1.90 Å [16]. The X-ray analyses of Mn(Pc), Fe(Pc) and Zn(Pc) show that the metals occupy the in-plane position and the radii of their cavities are 1.94 Å, 1.93 Å, and 1.98 Å respectively [27]. Here too, as in the case of Me(P) complexes, the metal position is not related to the ionic radii. (The discrepancy between the sum of metal and ligand ionic radii and the cavity radius in the case of Me(Pc) complexes is even larger than in case of Me(P) complexes.)

It follows that the Hoard assumption, that the out-of-plane position of the metal in metalloporphyrins is always preferable to the porphyrin ring distortion, is ungrounded. In addition, in this model the mechanism controlling the multiplicity (spin state) of the metal remains unclear. (Why, for instance, in the case of Mn(P) the high spin state of the metal is realized, whereas in the case of Mn(Pc) its state is of intermediate spin [27a,28]?)

However, as shown in Section B, the question whether the in-plane position of the metal in complexes is stable or not is a typical vibronic problem which can be solved directly by using the criterion of instability (eqn. (5) or (7)) with respect to out-of-plane nuclear displacements. In order to fulfil the inequality (5) an excited state Ψ_2 is needed, for which the vibronic constant F of its mixing with the ground state Ψ_1, as in eqn. (3), is non-zero and large enough. It is shown in this section that, on the basis of a rigorous vibronic approach, a non-contradictory description of the structure and properties of metalloporphyrins is achieved, which can explain the experimental data concerning both geometries and spin states.

(i) Adiabatic potentials for different electronic states [29]

We shall consider the energy scheme for the one-electron highest occupied MO (HOMO) and the lowest unoccupied MO (LUMO) for several 3*d* metalloporphyrins (Mn, Fe, Co, Ni, Cu, Zn) and manganese phthalocyanine (MnPc) [30–33] (Fig. 4). It is seen that low lying high spin states are present for Mn, Fe, Co and Ni only. In the case of Mn(P), Fe(P) and Co(P) the high spin state of lowest energy is formed by electron excitation from the $e_g(d_\pi)$ MO to $b_{1g}(d_{x^2-y^2})$, whereas in the case of $\mathrm{Ni^{II}}$(P) it can be obtained by an $a_{1g}(d_{z^2}) \rightarrow b_{1g}(d_{x^2-y^2})$ excitation. Thus all the states of interest can be divided into four qualitatively different classes: (1) with partially occupied $a_{1g}(d_{z^2})$ MO and empty $b_{1g}(d_{x^2-y^2})$ MO (the ground state of $\mathrm{Mn^{II}}$(P), $\mathrm{Mn^{II}}$(Pc), $\mathrm{Co^{II}}$(P), $\mathrm{Fe^{II}}$(P) and $\mathrm{Fe^{I}}$(P)); (2) with filled $a_{1g}(d_{z^2})$ MO and empty $b_{1g}(d_{x^2-y^2})$ MO (the ground state of $\mathrm{Ni^{II}}$(P), $\mathrm{Co^{I}}$(P) and $\mathrm{Fe^{0}}$(P)); (3) with filled $a_{1g}(d_{z^2})$ MO and fully or partially occupied $b_{1g}(d_{x^2-y^2})$ MO (the ground state of $\mathrm{Cu^{II}}$(P) and $\mathrm{Zn^{II}}$(P)); (4) with partially occupied $a_{1g}(d_{z^2})$

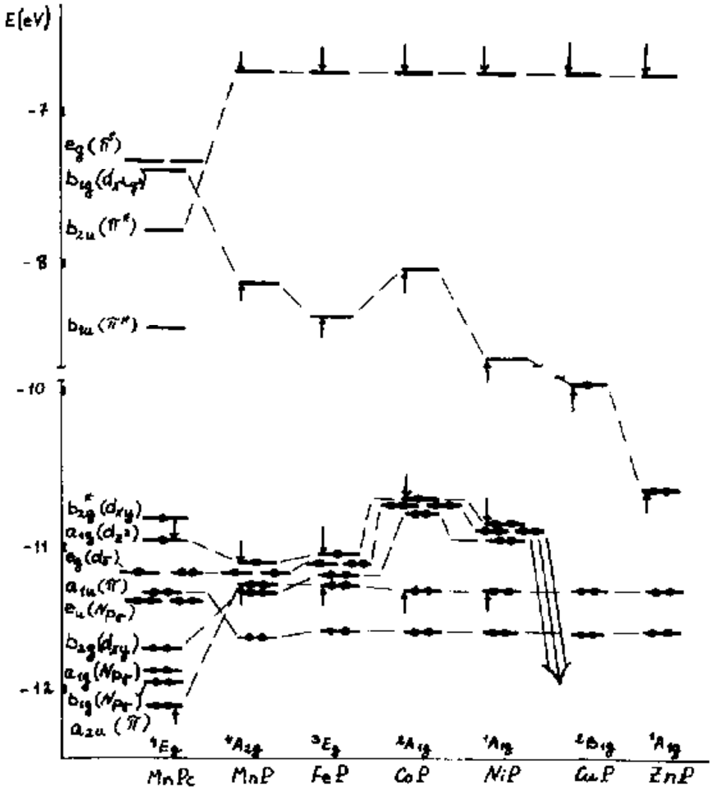

Fig. 4. Energy levels for the highest occupied and lowest unoccupied MO of manganese phthalocyanine [32] and metalloporphyrins [30,31,33].

and $b_{1g}(d_{x^2-y^2})$ MO (excited high spin states of $Mn^{II}(P)$, $Mn^{II}(Pc)$, $Fe^{II}(P)$, $Fe^{I}(P)$, $Fe^{0}(P)$, $Co^{II}(P)$, $Co^{I}(P)$ and $Ni^{II}(P)$).

Now we shall consider qualitatively the shapes of the adiabatic potential surfaces for the electronic states of these four classes in the space of nuclear displacement driving the metal atom out of the plane of the porphyrin (phthalocyanine) ring. Since the symmetry of the systems in the metal-in-plane configuration is D_{4h}, the out-of-plane displacement of the metal atom is of A_{2u} symmetry. This displacement mixes the ground electronic state with certain excited states having appropriate symmetries. In case (1) the lowest of such states (with the same multiplicity as the ground state) can be obtained by excitation of an electron from the $a_{2u}(\pi)$ MO to $a_{1g}(d_{z^2})$ ($A_{2u} \times A_{1g} = A_{2u}$). As a result of the vibronic mixing of the ground and excited electronic states their adiabatic potential energies have the form of eqn. (4), where q is the symmetrized A_{2u} displacement under consideration (for the metal in-plane position $q = 0$), 2Δ is the energy gap between the mixing electronic states, K_0 is the force constant of the A_{2u} displacement (without taking account of vibronic mixing) and F is the vibronic mixing constant specified above.

If the criterion of instability (eqn. (5)) is fulfilled, then the in-plane position of the metal is unstable, and if the Me(P) is chemically stable, then the minima (stable configurations) are displaced to the points (Fig. 1)

$$\pm q_0 = \pm \left(\frac{F^2}{K_0^2} - \frac{\Delta^2}{F^2} \right)^{1/2} \tag{9}$$

The energy at these points is

$$E_{1,\min} = -\frac{\Delta}{2} \left(\frac{F^2}{K_0 \Delta} + \frac{K_0\,\Delta}{F^2} \right) \tag{10}$$

In case (2) there are no low lying excited states which are admixed with the ground state by A_{2u} displacements. Thus the ground state at $q = 0$ is not softened by the vibronic interactions.

In case (3), according to ref. 14, the population of the $b_{1g}(d_{x^2-y^2})$ MO results in the metal being in plane and accompanied by an increase in the radius of the porphyrin ring cavity by about 0.1 Å. Therefore in order to determine the equilibrium configuration in this case, the interaction with totally symmetric A_{1g} displacements has also to be taken into account [1]. We denote them here by q' and the appropriate vibronic constant by F' (q' will be read off from the geometry of complexes with unoccupied $b_{1g}(d_{x^2-y^2})$ MO).

It is easily seen from Fig. 4 that the only low lying state which mixes with the ground state under A_{2u} displacements in class (3) of the states is that obtained by a one-electron excitation $b_{1g}(d_{x^2-y^2}) \rightarrow b_{2u}(\pi^*)$. The vibronic interaction of these two states described by the vibronic constant F_0, is assumed to be relatively small. This assumption is based on X-ray experiments [34–36] showing that for all the metalloporphyrins with in-plane positions of the metal atom the mean square amplitude of the metal out-of-plane vibrations (and hence elasticity constants) do not differ by more than 10%–20%. Direct calculation of the adiabatic surface of Fe(P) [37] does not agree with these experimental data. Considering the interaction with both $A_{1g}(q')$ and $A_{2u}(q)$ displacements we obtain (cf. eqn. (4))

$$E_3(q, q') = -\Delta + F'q' + \frac{K'(q')^2}{2} + \frac{1}{2}\left(K_0 - \frac{F_0^2}{\delta}\right)q^2 \tag{11}$$

which gives

$$q_0' = -F'/K'$$

$$q_0 = 0 \tag{12}$$

and

$$E_{3,\min} = -\Delta - \frac{(F')^2}{2K'} \tag{13}$$

Here $-\Delta$ is the energy of the state under consideration at $q' = 0$ and $q = 0$, $2\ \delta$ is the energy gap to the excited state, K' and K_0 are the elasticity constants (force constants) for the A_{1g} and A_{2u} displacements respectively. It is seen that the interaction with the totally symmetric displacement A_{1g} results in a shift of the position of the minimum along the q' coordinate by $-F'/K'$ (the experimental data [14] yield $F' < 0$) and a lowering of its energy by $(F')^2/2K'$. The interaction with the A_{2u} displacements leads to a softening of the force constant K_0 in this direction (not resulting in instability since $(F_0^2/\delta) < K_0$, as assumed above).

For class (4), Ψ_1 are the excited states and their energy is denoted by $E - \Delta$. By the A_{2u} displacements these states mix with two upper states which are close in energy. The first, Ψ_2, is formed by an $a_{2u}(\pi) \rightarrow a_{1g}(d_{z^2})$ excitation, the state with the doubly occupied a_{1g} MO having the energy $E + \Delta$ (cf. class (1)). The vibronic constant of mixing of these two states, F, coincides with that of class (1). The second upper excited state, Ψ_3, is appropriate to a $b_{1g}(d_{x^2-y^2}) \rightarrow b_{2u}(\pi^*)$ excitation (cf. class (3)). The energy of the Ψ_3 state is $E + 2\ \delta - \Delta$, its mixing with Ψ_1 being characterized by the same vibronic constant F_0 as in the case of class (3) (since it is mixing of the same electronic states by the same nuclear displacements).

Let us consider now the interaction of these states with both A_{1g} and A_{2u} displacements. Following the reasoning given above for classes (1) and (3), we consider the mixing of the states Ψ_1 and Ψ_2 exactly, while the mixing of Ψ_1 and Ψ_3 by the same displacements will be taken into account as a perturbation. In this approximation the adiabatic potentials of the states under consideration are eigenstates of the following matrix:

$$\begin{vmatrix} E-\Delta+F'q'+\tfrac{1}{2}K'(q')^2+\tfrac{1}{2}K_0q^2-\dfrac{1}{2\,\delta}F_0q^2 & Fq \\ Fq & E+\Delta+F'q'+\tfrac{1}{2}K'(q')^2+\tfrac{1}{2}K_0q^2 \end{vmatrix} \tag{14}$$

from which we obtain

$$E_4(q', q) = E + F'q' + \tfrac{1}{2}K'(q')^2 + \tfrac{1}{2}K_0q^2 + \frac{1}{4}\,\frac{F_0q^2}{\delta} - \left[\left(\Delta + \frac{F_0^2q^2}{4\delta}\right)^2 + F^2q^2\right]^{1/2} \tag{15}$$

From this equation it follows that the minima of the adiabatic potential lie at the points

$$q_0' = -F'/K'$$

$$q_0^2 = 2\frac{\Delta}{K_0}\,\frac{[\alpha(\alpha+2\beta)(1-\beta)]^{1/2}-(\alpha+\beta)}{\beta^2} \tag{16}$$

$$\alpha = F^2/K_0\,\Delta;\ \beta = F_0^2/2K_0\delta \tag{17}$$

and the condition (necessary and sufficient) for instability of the system at $q=0$ is

$$\frac{F^2}{\Delta} + \frac{F_0^2}{\delta} > K_0 \tag{18}$$

(cf. eqn. (7)).

The energy at the minimum point (cf. the Jahn–Teller stabilization energy [1] (Fig. 1)) is as follows:

$$E_{4,\min} = E - \frac{(F')^2}{2K'} - \Delta\frac{(1-\beta)(\alpha+\beta)-[\alpha(\alpha+\beta)(1-\beta)]^{1/2}}{\beta^2} \tag{19}$$

Thus in the framework of the approximations employed above, we obtained the qualitative features of the adiabatic potentials in all four classes of possible electronic states in the systems under consideration. It allows us to pass to the solution of the problem of ground state multiplicity and geometry.

(ii) Ground state multiplicity and geometry

If the ground state of the metalloporphyrin with a planar configuration possesses an intermediate spin, then by an out-of-plane displacement of the metal atom, the high spin state can become the ground state if its energy decreases faster by this displacement than that of the intermediate spin. It follows from eqns. 10, 14 and 19 that such a situation is quite possible, since the high spin state has a reduced force constant compared with that of the intermediate spin state owing to the vibronic mixing with the next excited state Ψ_3.

Concerning the nature of the intersection of the above two terms of different multiplicity, two situations must be distinguished.

(a) Only the high spin term is vibronically unstable, i.e. the relation (18) is obeyed, whereas the relation (5) is not valid. In this case the high spin term becomes the ground state when the Jahn–Teller stabilization energy is greater than the excitation energy at $q = 0$ (Fig. 5(a)).

(b) Both terms under consideration are unstable (both inequalities (5) and (18) are obeyed). In this case the high spin term becomes the ground state upon distortion, if its Jahn–Teller stabilization energy is larger than the sum of that of the intermediate-spin state and of the energy of excitation at $q = 0$ (Fig. 5(b)).

This consideration explains a series of experimental data. Indeed, as seen in Fig. 4, most softening, or even instability, of the in-plane position of the metal atom is expected for $\mathrm{Mn^{II}(P)}$ and $\mathrm{Fe^{II}(P)}$ whose empty or partially occupied $a_{1g}(d_{z^2})$ orbital produces the lowest Δ value for these systems. In $\mathrm{Mn^{II}(Pc)}$ the Δ value is much larger than in $\mathrm{Mn^{II}(P)}$, which results in an inversion of the inequality (5) and explains why the Mn atom in $\mathrm{Mn^{II}(Pc)}$ occupies the in-plane position [27] in spite of the fact that in phthalocyanine the internal cavity is 0.2 Å smaller than in porphyrin. As noted at the beginning of this section, from the point of view of the requirement of

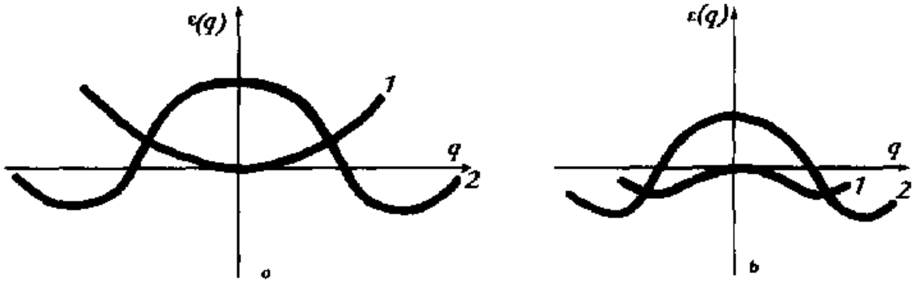

Fig. 5. The mutual positions of the adiabatic curves for intermediate or low (curve 1) and high (curve 2) spin states in the cases when the former is stable (a) and unstable (b) at $q = 0$.

correspondence between the radius of the metal atom (or ion) and the dimensions of the cavity [13,16,20], the fact that the Mn atom in $Mn^{II}(Pc)$ occupies the in-plane position was not understood. Within the vibronic approach, these (and other) facts acquire a natural explanation.

Similarly, the in-plane position of the metal atom in Zn(P) and Ag(P) observed experimentally [24,25,38,39] can be explained. Indeed, because the mixing of the $b_{1g}(d_{x^2-y^2})$ and $b_{2u}(\pi^*)$ orbitals by A_{2u} displacements is weak, the inequality $(F_0^2/\delta) > K_0$ is not fulfilled and the in-plane position of the metal, although slightly softened, remains stable, whereas the increase in the metal dimensions by population of the $b_{1g}(d_{x^2-y^2})$ MO results in a totally symmetric deformation of the porphyrin ring. In the case of $Ni^{II}(P)$, $Co^{I}(P)$ and $Co^{0}(P)$ the ground state has a filled $a_{1g}(d_{z^2})$ MO and a vacant $b_{1g}(d_{x^2-y^2})$ MO, and thus the in-plane position of the metal is not even softened by the vibronic interactions.

The high spin $Ni^{II}(P)$ and low spin $Co^{II}(P)$ must be considered more carefully using numerical estimations of the parameters of the inequality (5). Indeed, with the vibronic constant F estimated for Fe(P) to be $F^2 \approx 0.25$ eV Å^{-2} [40–42] (for other appropriate $3d$ metalloporphyrins, F is expected to be of the same order of magnitude since it is determined by quite similar MOs), the force constant $K_0 \leq 1$ eV Å^{-2}, obtained in a series of theoretical [43] and experimental [44–46] studies, and with the values from refs. 30–33 and 47 (see Fig. 4), we conclude that for these compounds the inequality (5) is not obeyed and hence the metal in-plane position is stable. Thus for $Co^{II}(P)$, $Co^{I}(P)$, $Co^{0}(P)$ and $Ni^{II}(P)$ in their ground states, an in-plane configuration of the metal atom is expected in accordance with experimental data [34,35,48–51]. From this point of view, the calculation of the potential energy surface for $Co^{I}(P)$, predicting an out-of-plane position of the Co atom [52], remains unclear.

The origin of the high spin ground state of Mn(P) with the out-of-plane position of the Mn atom [28] can be understood to result from the strong vibronic mixing of this state with the excited state. It follows from eqns. (10) and (19) that the high spin state is the ground state, if the following inequality is valid:

$$E - \frac{(F')^2}{2K'} - \Delta\frac{(1-\beta)(\alpha+\beta) - [\alpha(\alpha+\beta)(1-\beta)]^{1/2}}{\beta^2} < -\frac{\Delta}{2}\left(\alpha + \frac{1}{\alpha}\right) \tag{20}$$

It can easily be shown that this inequality is obeyed when the parameter $\alpha = F^2/(K_0\,\Delta)$ is large enough, which ceteris paribus requires a small energy gap Δ to the excited state. As seen from Fig. 4, the Δ value is indeed the smallest for Mn(P).

Finally, let us compare the theoretical predictions of the vibronic theory with the experimental data for the most studied case, namely Fe(P). According to the above mentioned estimates of the parameter values in the inequality (5), the relation $F^2/(K_0 \Delta) \approx 1$ is valid. Therefore, first, the inequality (20) is not fulfilled and hence the ground state is expected to have intermediate spin. Secondly, for an empty or partially filled d_{z^2} orbital, this state is either softened (with the adiabatic potential minimum at $q = 0$) or unstable with two shallow minima (with a small Jahn–Teller stabilization energy); in both cases the in-plane position of the Fe atom in $Fe^{II}(P)$ is very soft; this result is also important for the analysis of the spatial configuration in the presence of axial ligands given in the next section.

As seen from Fig. 4 in the case of $Fe^{II}(P)$, the lowest intermediate-spin state can be either ${}^3A_{2g}[(xy)^2(xz)^1(yz)^1(z^2)^2]$ or ${}^3E_g[(xy)^2(xz, yz)^3(z^2)^1]$. With the term ${}^3A_{2g}$, the d_{z^2} orbital is completely occupied and therefore the in-plane position of the iron atom is stable and not softened. On the contrary, in the ${}^3E_g$ state the in-plane configuration is either strongly softened or even slightly unstable. Direct quantum-chemical calculations [53–58] of the planar $Fe^{II}(P)$ show that the ground state in this configuration is ${}^3A_{2g}$ with the ${}^3E_g$ state somewhat higher in energy. This result is confirmed by magnetic susceptibility measurements [59], nuclear magnetic resonance [59,60] and the Mössbauer effect [61]. X-ray analysis [62] is also in favour of the filled $a_{1g}(d_{z^2})$ orbital in the ground state.

The only experimental results which disagree with this statement are those obtained by resonance Raman scattering in Fe^{II}(OEP) [63]. In this work, it is claimed that the ground state is ${}^3E_g$, since the frequency of the IV Raman band, indicating the magnitude of electronic charge transfer from the metal to the porphyrin states, is near to the frequency of the low spin system $Fe^{III}(OEP)(Im)_2$. The number of d_π electrons is three, and the frequency differs from the frequencies of compound II of horse-radish peroxidase where the number of d_π electrons is two. Three d_π electrons determine the ${}^3E_g$ term, whereas in the ${}^3A_{2g}$ term there are only two electrons. However, it should be noted that the transfer of d_π electrons from the metal to the π states of the porphyrin ring depends not only on the number of d_π electrons on the metal atom, but also on the nature of the axial ligands. Therefore the conclusion [63] about the ${}^3E_g$ ground state in the Fe^{II}(OEP) is questionable, especially when compared with the other data listed above.

Assuming that the ground state of $Fe^{II}(P)$ is ${}^3A_{2g}$, the iron atom occupies an in-plane position in agreement with X-ray investigations [64,65]. The planar configuration of $Fe^{II}(P)$ is also consistent with the ${}^3E_g$ ground state with the reservation that in this case the A_{2u} vibrations have to be of much lower frequencies than in the case of the ${}^3A_{2g}$ state. It follows that $[Fe(P)]^-$ and $[Fe(P)]^{2-}$ also have a planar configuration. Indeed, the addition of electrons to the $Fe^{II}(P)$ systems either influences the population of the d_{z^2} orbital making it fully occupied, or changes the population of the other MO not involved in the formation of the nuclear configuration under consideration. In both cases the resulting state leaves the metal in-plane configuration undistorted in agreement with experimental data [66].

The origin of the stable nuclear configuration of Fe(P) was also investigated by direct quantum-chemical calculations [53,56,67]. It was shown that in all the electronic states studied the in-plane position of the iron atom is stable, but the force constant for the A_{2u} frequency varies from state to state.

The vibronic origin of possible out-of-plane displacements of the iron atom in Fe(P) was also considered by Mizuhashi [68–71]. Starting from the same idea of the importance of vibronic interactions in this problem, the approach in refs. 68–71 differs from that described above, in that it is assumed that the contribution to the instability of the planar configuration is due to mixing of the pure atomic states of iron arising from its different electronic configurations, namely a mixture of the $3d^6$ and $3d^5 4p$ configurations. This means that only the effect of polarization of the atomic shells by nuclear displacements is taken into account. This approach cannot be considered satisfactory, since, as shown in Section B, the polarization contribution is smaller by an order of magnitude than the main contribution, which is due to the effect of formation of new covalent bonds by the nuclear displacements (covalent contribution). Therefore it is not surprising that in the Mizuhashi model (polarization approach) a variety of data on different metalloporphyrins cannot be explained. In particular, the origin of the well-known planar configurations in Ni(P), Cu(P), Zn(P) and Ag(P) cannot be understood in this model. Moreover, the calculations of the magnitude of mixing using eqn. (4) of ref. 70 results in an overestimate of the vibronic mixing constants and hence in an underestimate of the resulting force constants [70,71]. Apparently, this is the reason for the conclusion that the planar configurations are unstable in all low lying electronic states of $Fe^{II}(P)$ [70,71] in contrast with experimental data [64,65]. Also ungrounded seems to be the estimate of the initial (non-vibronic [1]) A_{2u} force constant K_0 in refs. 69–71. It is smaller by an order of magnitude than that given in ref. 69 for the iron–nitrogen interaction. (It is seen from Fig. 3 of ref. 69 that the main contribution to the frequency of the vibration comes not from the displacement of the iron atom, but from the non-planar displacements of the porphyrin ring atoms.)

To summarize this section, the experimental data on the geometry and electronic ground state multiplicity of $3d$ metalloporphyrins are satisfactorily explained by means of the vibronic approach in which the mixing of the $a_{1g}(d_{z^2})$ and $a_{2u}(\pi)$ MOs by out-of-plane metal displacement plays a key role.

D. STEREOCHEMISTRY OF METALLOPORPHYRIN AND HEMOPROTEIN ACTIVE CENTRE COMPLEXES WITH AXIAL LIGANDS

In this section the vibronic approach is used to elucidate the geometry and stereochemistry of metalloporphyrins with one or two axial ligands, and of hemoprotein active centres in the deoxy form, as well as their complexes with different ligands.

(i) Perturbation theory for geometry changes by coordination

There are several versions of the perturbation theory aimed at the investigation of chemical reactivity [72–75]. In application to the change of molecular geometry by chemical bonding such a version of perturbation theory, to our knowledge, was first reported in refs. 76 and 77. (A related problem of the mutual influence of ligands in simple complexes was considered earlier [78–80].) In this subsection, the version of perturbation theory under consideration is illustrated by its application to the case of three interacting subsystems (reagents).

We present the Hamiltonian of the system in the form

$$H = H_0 + W \tag{21}$$

where

$$H_0 = H_0^{\mathrm{P}} + H_0^{\mathrm{L}_1} + H_0^{\mathrm{L}_2} + H^{\mathrm{PL}_1} + H^{\mathrm{PL}_2} \tag{22}$$

and H_0^{P}, $H_0^{\mathrm{L}_1}$ and $H_0^{\mathrm{L}_2}$ are the Hamiltonians of the non-interacting subsystems P, L_1 and L_2 in some fixed stable (with respect to totally symmetric nuclear displacements) configurations. H^{PL_1} and H^{PL_2} are the components of the interaction operators of the subsystems P and L_1, and P and L_2 respectively, which are diagonal with respect to the eigenfunctions of the operator $H_0^{\mathrm{P}} + H_0^{\mathrm{L}_1} + H_0^{\mathrm{L}_2}$; W denotes

$$W = H_{\mathrm{PL}_1} + H_{\mathrm{PL}_2} + H_{\mathrm{v}} \tag{23}$$

where H_{PL_1} and H_{PL_2} are the electronic non-diagonal (in the sense given above) parts of the interaction between the subsystems, and H_{v} is the operator of the vibronic interactions with non-totally symmetric displacements within each of the subsystems.

For the sake of simplicity we assume that the interaction between L_1 and L_2 can be neglected. Since we are interested only in the influence of all the interactions under consideration upon the geometry of one subsystem P, we consider the vibronic interactions within this P system only.

The perturbation problem can be reduced to the following secular equation:

$$\| H_{ij} - ES_{ij} \| = 0 \tag{24}$$

Its solution can be obtained by the matrix representation of the Hamiltonian (eqn. 21) built up by the eigenfunctions of the zeroth order operator $H_0^{\mathrm{P}} + H_0^{\mathrm{L}_1} + H_0^{\mathrm{L}_2}$. (It should be noted that the MOs are orthonormalized only within each of the subsystems, thus being non-orthogonal between the subsystems.)

To solve eqn. (24) we use the perturbation theory with respect to the operator W. The first non-vanishing correction to the ith MO owing to the vibronic interactions within P and non-diagonal interactions between the subsystems is the following second-order perturbation correction:

$$E_i^{(2)} = -\sum_j \frac{\left(W_{ij} - E_i^{(0)} S_{ij}\right)^2}{E_j^{(0)} - E_i^{(0)}} \tag{25}$$

Considering only one non-totally symmetric coordinate of vibronic interaction q (in the absence of interactions, $q = 0$) and denoting

$$\langle i \,|\, H_{\mathrm{PL}_1} \,|\, j \rangle = A_{ij}$$

$$\langle i \,|\, H_{\mathrm{PL}_2} \,|\, j \rangle = B_{ij}$$

$$\langle i \,|\, H_{\mathrm{v}} \,|\, j \rangle = f_{ij} q \tag{26}$$

we deduce from eqn. (23), that for different i and j, the matrix element W_{ij} acquires the values given in Table 1.

The change in the total energy is approximately equal to the sum of the energy corrections to each MO (eqn. (25)) multiplied by their occupation numbers. In this sum the terms describing the interaction of fully occupied orbitals vanish, since they occur twice with opposite signs (in the nominator $W_{ij} = W_{ji}$, the denominators have opposite signs).

TABLE 1

The matrix elements W_{ij} for different i and j values of the wavefunctions

i	j		
	$j \in P$	$j \in L_1$	$j \in L_2$
$i \in P$	$f_{ij}Q + A_{ij} + B_{ij}$ $(S_{ij} = 0)$	A_{ij}	B_{ij}
$i \in L_1$	A_{ij}	A_{ij} $(S_{ij} = 0)$	0
$i \in L_2$	B_{ij}	0	B_{ij} $(S_{ij} = 0)$

Thus the expression for the energy as a function of the q displacement is as follows:

$$E(q) = E_0 + \mathscr{D} + \tfrac{1}{2}K_0 q^2 - \tfrac{1}{2}q^2 \sum_{i,j} \left(p_i f_{ij}^2 / \Delta_{ji} \right) - q \sum_{i,j} \left[p_i f_{ij} (A_{ij} + B_{ij}) / \Delta_{ji} \right] \tag{27}$$

where i and j label the functions of the subsystem P, p_i is the occupation number of the ith MO

$$2\Delta_{ij} = E_i^{(0)} - E_j^{(0)} \tag{28}$$

and $K_0 q^2/2$ is the elastic energy for the q displacement in the P subsystem; $\mathscr{D}$ denotes the pure electronic corrections independent of q. Assuming

$$K_0 > \sum_{i,j} \left(p_i f_{ij}^2 / \Delta_{ji} \right) \tag{29}$$

we obtain that the equilibrium geometry of the P subsystem as a result of interactions between the three subsystems (and vibronic interactions within P) changes from $q = 0$ to

$$q_0 = \frac{\sum_{i,j} \left[p_i f_{ij} (A_{ij} + B_{ij}) / \Delta_{ji} \right]}{K_0 - \sum_{i,j} \left(p_i f_{ij}^2 / \Delta_{ji} \right)} \tag{30}$$

It should be noted that the nature of instability of the P subsystem at $q = 0$ obtained here is different from that obtained in Sections B and C. Indeed, in these cases the instabilities are dynamic in nature (i.e. they correspond to the maximum of the adiabatic potential where the first derivatives, the forces, equal zero) and take place only when the condition of strong vibronic interaction (eqn. (5)) is obeyed. However, in the case under consideration in this section the instability at $q = 0$ is static in nature, i.e. it arises due to a non-zero force and almost always takes place. There are two exceptions: the first if

$$A_{ij} + B_{ij} = 0 \tag{31}$$

and the second if

$$f_{ij} = 0 \tag{32}$$

It is obvious that the condition given by eqn. (32) cannot occur for any i and j since from symmetry considerations for any ith MO there can be such an excited j which mixes with the ith MO under the q displacements. However, if the j state is high in energy, then Δ_{ij} is large and the distortion (eqn. (30)) is small. Equation (31) can be obeyed for any i and j for certain symmetries of the complex and the displacement (see below). In this case the distortion of the P geometry can be due only to its dynamic instability at $q = 0$, i.e. when the inequality, inverse to eqn. (29), takes place. It should be noted that in the presence of interactions with L_1 and L_2 the inequality (29) is different from that expected for the free P system owing to changes in the Δ_{ij} values (by interaction) already in the zeroth order Hamiltonian (eqn. (22)).

The nature of the A_{ij} and B_{ij} parameters of eqns. (27) and (30) will now be considered. As we can see from eqn. (26) and Table 1, the A_{ij} and B_{ij} values characterize the influence of the ligand-field charges of the subsystems L_1 and L_2 on the electronic structure of the P subsystem. In this meaning the A_{ij} and B_{ij} parameters are analogous to the appropriate crystal-field approximations [5,81]. It also follows from eqn. (27) that, when q is non-degenerate, the sum $A_{ij} + B_{ij}$ has the same transformation properties as q. In particular, if the crystal field of the subsystems L_1 and L_2 is totally symmetric, the term in eqn. (27) which is linear in the non-totally symmetric displacement q equals zero.

(ii) Application to the spin state / metal position relationship

In this subsection we use the perturbation theory version, considered above, to investigate the relationship between the out-of-plane displacement q of the metal atom from the porphyrin ring and the number and nature of axial ligands. Thus in the formulae of the previous subsection, L_1 and L_2 are the first and second axial ligands and P is a metalloporphyrin. In the application of eqns. (27)–(30) the mixing of only the highest occupied MOs (HOMO) and lowest unoccupied MOs (LUMO) of the metalloporphyrins (including the $4p$ orbital of the metal) will be taken into account since, as shown above, the contributions of the MO mixing, other things being equal, are inversely proportional to the energy gap between them.

The crystal-field contributions of the axial ligands transform as the irreducible representations of the D_{4h} group. As indicated above, the metal out-of-plane displacement under consideration transforms as the A_{2u} representation. Therefore only the A_{2u} component of the crystal field of the ligands gives non-zero contributions to the matrix elements A_{ij} and B_{ij}, its totally symmetric component being included in the zeroth order Hamiltonian (eqn. (22)). Thus non-zero matrix elements A_{ij} and B_{ij} can be obtained for the following pairs of MOs: $a_{1g}(d_{z^2})$ and $a_{2u}(\pi)$, $b_{1g}(d_{x^2-y^2})$ and $b_{2u}(\pi^*)$, $e_g(d_\pi)$ and $e_u(4p_\pi)$, $a_{1g}(d_{z^2})$ and $a_{2u}(4p_z)$; hence the mixing of the orbitals within these pairs results in an out-of-plane displacement of the metal atom from the porphyrin ring.

Equations (27) and (30) were obtained under the condition given by eqn. (29). This condition is valid for the complexes Co(P), Ni(P), Cu(P) and

Zn(P). Indeed, in these metalloporphyrins without axial ligands, as shown in Section C, the criterion of pseudo-Jahn–Teller instability (the inequality inverse to eqn. (29)) is not valid. By ligand coordination the energy gap Δ_{ij} between the $a_{2u}(\pi)$ and $a_{1g}(d_{z^2})$ MOs increases (owing to the totally symmetric component of the crystal field), while that between the $b_{1g}(d_{x^2-y^2})$ and $b_{2u}(\pi^*)$ MOs is almost unaffected. As a result, the planar configuration becomes dynamically more stable.

For the complexes Fe(P) and Mn(P) we assume (see also ref. 47) that, owing to interactions with the totally symmetric component of the ligand crystal field increasing the Δ_{ij} values, the metal in-plane configuration becomes dynamically stable at $q = 0$. This assumption is strengthened by the fact that the instability criterion at $q = 0$ (eqn. (18)), as well as the criterion of term crossing (eqn. (20)), is very sensitive to the interaction with the axial environment (see Section C).

(a) Complexes with one axial ligand

Complexes with one axial ligand in which the metal atom is five-coordinated will be considered now in more detail. In this case, $B_{ij} = 0$ and eqn. (30) transforms to

$$q_0 = \frac{\sum_{i,j} \left(p_i f_{ij} A_{ij} / \Delta_{ji} \right)}{K_0 - \sum_{i,j} \left(p_i f_{ij}^2 / \Delta_{ji} \right)} \tag{33}$$

The energy of the system at this point equals

$$E(q_0) = E_0 + \mathscr{D} - \frac{1}{2} \frac{\left[\sum_{i,j} \left(p_i f_{ij} A_{ij} / \Delta_{ji} \right) \right]^2}{K_0 - \sum_{i,j} \left(p_i f_{ij}^2 / \Delta_{ji} \right)} \tag{34}$$

The stabilization energy (the reduction in the energy due to the metal out-of-plane displacement q_0) is

$$\Delta E = \frac{1}{2} \frac{\left[\sum_{i,j} \left(p_i f_{ij} A_{ij} / \Delta_{ji} \right) \right]^2}{K_0 - \sum_{i,j} \left(p_i f_{ij}^2 / \Delta_{ji} \right)} \tag{35}$$

We shall consider now complexes of different metalloporphyrins. It follows from general considerations that the orbitals most mixed by external fields are pairs of MOs (from those listed above), which are directed perpendicular to the porphyrin ring, the mixing being the more effective the closer to each other and to the ligand are their electron densities. Hence the maximum values of A_{ij} are expected for the following pairs of MOs: $a_{2u}(\pi)$ and $a_{1g}(d_{z^2})$, and $a_{1g}(d_{z^2})$ and $a_{2u}(4p_z)$. However, the smallest appropriate elasticity constants are expected for complexes with partially occupied $a_{1g}(d_{z^2})$ and $b_{1g}(d_{x^2-y^2})$ MOs. It follows that the largest metal displacements q_0 (eqn. (33)) are expected only for compounds with partially filled $a_{1g}(d_{z^2})$ and $b_{1g}(d_{x^2-y^2})$ orbitals. Indeed, the largest displacements of the metal atom are observed in the high spin complexes of Fe(II), Fe(III) and Mn(II) [14] which obey these conditions. The same effect explains the smaller out-of-plane displacement of the metal, Mn–Ct = 0.27 Å, in $\mathrm{Mn^{III}(TPP)(Cl^-)}$ ($S = 2$) [82] than in $\mathrm{Fe^{III}(TPP)(Cl^-)}$ ($S = 5/2$), where Fe–Ct = 0.39 Å [83], since in the former case the $b_{1g}(d_{x^2-y^2})$ MO is unoccupied, whereas in the latter case it is occupied.

It follows also from this discussion that the interaction of the d_{xy}, d_{xz} and d_{yz} orbitals with the metal out-of-plane displacements is weak, and therefore the population of these orbitals, other things being equal, does not affect the magnitude of this displacement. In particular, the change in the charge state of the iron atom, Fe(II) → Fe(III), is expected to result in rather small changes in the magnitude of the out-of-plane displacement. The differences in the dimensions of the iron ions in ferri- and ferro-complexes, as in the case of metalloporphyrins without axial ligands, is thus expected to influence only the dimensions of the ring cavity and not the out-of-plane Me–Ct distance. This result is confirmed by the experimental data on the stereochemistry of iron porphyrin complexes with one axial ligand [83], which show explicitly that the reduction of the iron ion charge by unity increases essentially the dimensions of the cavity and does not influence the Fe–Ct distance at all. These data are incomprehensible in the framework of the Hoard model [18].

We shall now consider the influence of the axial ligand on the multiplicity of the ground state of the metalloporphyrins using Fe(P) and Mn(P) as examples. With eqns. (33) and (34) we easily obtain the following expression for the difference in energies at the minima configurations for high, intermediate and low spin ground states:

$$\begin{aligned} &E^h(q_0^h) - E^{i(l)}(q_0^{i(l)}) \\ &\quad = E^h(0) - E^{i(l)}(0) \\ &\qquad - \tfrac{1}{2}\left[q_0^h \sum_{i,j} \left(p_i^h f_{ij} A_{ij}/\Delta_{ji} \right) - q_0^{i(l)} \sum_{i,j} \left(p_i^{i(l)} f_{ij} A_{ij}/\Delta_{ji} \right) \right] \qquad (36) \end{aligned}$$

The upper indices h, i and l denote the high, intermediate and low spin states respectively. It should be noted that the expression in the square brackets of eqn. (36) is always positive since in the high spin state the $a_{1g}(d_{z^2})$ and $b_{1g}(d_{x^2-y^2})$ orbitals are partially populated, thus resulting in a higher stabilization energy by distortion. Hence the out-of-plane displacement of the metal atom leads to a decrease in the energy gap between the states of high spin and intermediate (or low) spin. If the inequality

$$q_0^h \sum_{i,j} \left(p_i^h f_{ij} A_{ij} / \Delta_{ji} \right) - q_0^{i(l)} \sum_{i,j} \left(p_i^{i(l)} f_{ij} A_{ij} / \Delta_{ji} \right) > 2\left[E^h(0) - E^{i(l)}(0) \right] \qquad (37)$$

applies, the high spin state becomes the ground state; the greater the value of q_0, the more probable that the high spin state becomes the ground state.

Some care has to be taken when the magnitudes of distortion q_0 and state multiplicities are compared for metalloporphyrins with and without axial ligands. Indeed, the additional ligand produces a diagonal component of the crystal field which shifts the MO energies (mainly of the $a_{1g}(d_{z^2})$ and $a_{2u}(4p_z)$ type). As seen from the energy scheme in Fig. 4, for all the 3*d* metalloporphyrins except Ni(P), this shift increases the energy gap between the low (or intermediate) spin state and the high spin state.

Thus the addition of one ligand to the metalloporphyrin results in two competing effects determining the ground state multiplicity: the first effect produced by the non-diagonal crystal field promotes the out-of-plane displacement of the metal atom and lowers the energy of the high spin state, and the second effect, which is due to the diagonal component of the crystal field, increases the energy of the high spin (and even intermediate spin) state with respect to the low spin state and decreases the vibronic reduction of the A_{2u} force constant, thereby resulting in a decrease in the q_0 value.

It follows from the above arguments that the high spin ground state can be realized only in the case of weak-field ligands, i.e. ligands such as imidazole and mercaptide which produce small changes in the energy spectrum of the system Δ_{ij} [30,47,84,85]. In the case of ligands with a strong diagonal component of the crystal field (and small non-diagonal component), a low spin ground state with a not so large q_0 value is expected (see eqn. (38)). Examples of strong-field ligands include $C_6H_5^-$, CS, O_2 and NO. Their coordination, although favouring an out-of-plane displacement of the metal atom, produces a low spin ground state [13,14,76,77,83,86–94].

We shall consider next the influence of the same ligand on the out-of-plane displacements of the metal atom in metalloporphyrins of different metals (Mn, Fe, Co). The f_{ij} values (Section C) and Δ_{ij} magnitudes (Fig. 4) change weakly when passing from one compound to another in this series.

Therefore the change in the q_0 value is determined by the change in A_{ij}. The more the axial orbitals of the metal atom are extended in the direction of the ligand, the greater the magnitude of the matrix element of the non-diagonal crystal field. It is known [31] that the extent of the $a_{2u}(4p_z)$

and $a_{1g}(d_{z^2})$ orbitals decreases in the following sequence: Mn > Fe > Co. Hence the magnitude of the metal out-of-plane displacement in the series Mn(P), Fe(P), Co(P) with one axial ligand has to decrease in the same order. This conclusion is confirmed by experimental data [14] showing that in complexes with NO the distances from Mn, Fe, Co to the ring plane equal 0.34 Å, 0.21 Å and 0.09 Å respectively, while in the complexes of metalloporphyrins of the same metals with imidazole these distances change to 0.52 Å, 0.42 Å and 0.13 Å respectively. The fact that the metal displacement is smaller in complexes with NO than in those with imidazole, is because the crystal field of NO has a stronger diagonal component than that of imidazole, resulting also in the low spin ground state in the complex with NO.

It should be noted that the steric repulsion between the nitrogen atom of the NO group and the nitrogen atom of the pyrrole rings increases in the order Co < Fe < Mn [14,94] promoting the increase in the Me–Ct distance in the same order as the vibronic interaction. On the contrary, in complexes with substituted imidazoles the steric hindrance is stronger in (2-MeIm)Fe(P) than in (1-MeIm)Mn(P), whereas the Me–Ct distance is larger by 0.1 Å in the latter case than in the former [14]. This comparison confirms that in the out-of-plane displacement of the metal atom from the porphyrin ring, the vibronic effects are of primary importance and prevail over the hindrance effects.

The same vibronic approach can be used to explain the origin of the out-of-plane position of the metal atom in hemoprotein active centres. As a rule, the magnitude of the metal out-of-plane displacement here does not differ much from that of metalloporphyrins and model compounds [19,20,25,26,95–99]. At the same time the stronger the vibronic softening of the in-plane iron position, the greater the influence of the protein on the heme stereochemistry [100–103]. Following from the discussion above, the multiplicity of the ground state of the heme is determined not only by the metal atom position with respect to the plane of the porphyrin ring, but also by the strength of the crystal field of the proximal ligand which depends on the orientation of the latter, the distance to the metal atom [104,105] and the measure of protonation [106–108].

(b) Complexes with two axial ligands

Two equal axial ligands will be considered first. In this case, eqn. (31) is obeyed by symmetry considerations. Indeed, the sum of two identical fields within the point group symmetry D_{4h} transforms as the totally symmetric representation, and hence the non-totally symmetric part described by eqn. (31) equals zero. Hence, if the system is dynamically stable at $q = 0$ (i.e. if the inequality (29) is valid), its distortion in the case of two identical ligands is $q_0 = 0$. In the opposite case (when the inequality (29) is reversed) two

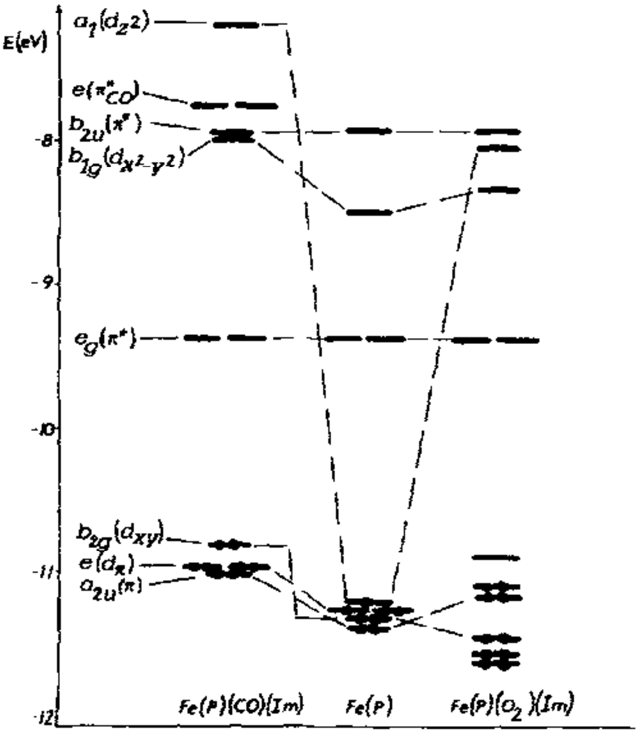

Fig. 6. Energy levels for the highest occupied and lowest unoccupied MO of ferroporphyrin complexes with [47] and without [31] axial ligands.

equivalent minima of the adiabatic potential are expected, for each of which the metal atom is in the out-of-plane position (on one or other side of the plane) with possible tunnelling between the two minima configurations (similar to the metalloporphyrin case without axial ligands).

If the two axial ligands are different, eqn. (31) is not valid, and there is a non-zero non-diagonal component of the crystal field producing a non-zero distortion, $q_0 \neq 0$, even when eqn. (29) is valid. However, in this case the magnitude of the metal out-of-plane displacement is expected to be smaller than in the case of one axial ligand. Indeed, in the case of two ligands, the diagonal part of the crystal field is stronger than in case of one ligand, producing a larger increase in the energy gap between the populated and empty MOs (Fig. 6). It should be noted that in the deoxy form of all hemoproteins (which are able to coordinate axial ligands) only one ligand, namely imidazole, tyrosine or mercaptide, is coordinated to the iron atom. The influence of the ligand on the active part of the energy spectrum is relatively small. On the contrary, the coordination of a strong ligand such as CO, NO and O_2 results in a sharp increase (more than an order of magnitude) in the gap between the $a_{2u}(\pi)$ and $a_{1g}(d_{z^2})$ orbitals (Fig. 6), and hence in an essential hardening of the iron atom out-of-plane vibrations.

This general conclusion is confirmed by experimental data on the coordination of CO to myoglobin [109]. It follows that the coordination of the above ligands, as second axial ligands, leads to a shift in the metal atom position toward the porphyrin plane (the steric effect also promotes this shift).

This conclusion agrees well with almost all experimental data on model compounds [13,14,83,94] and hemoproteins [19,20,105,108,110–127]. The complex of erythrocruorin with oxygen [100] is the only exception, the iron atom being displaced from the porphyrin ring by a distance 0.1 Å larger than in the deoxy form. The reason for this anomalous change in geometry under the influence of the protein globula may be due to some special interactions in this case which are not yet elucidated.

Following from the above discussion, the coordination of axial ligands with strong diagonal crystal fields leads to a ground state transition, high spin → low spin, in agreement with experimental data [13,14,19,20].

Thus the vibronic approach explains not only the fact of the metal out-of-plane displacement in the deoxy form of hemoproteins, but also its return toward the porphyrin ring (and even its return into the porphyrin plane) by coordination of strong ligands resulting in particular in the T → R conformational transitions in hemoglobin. In this case, the stronger the field produced by the coordinated ligand (the larger the energy gaps $\Delta_{a_{1g},a_{2u}}$), the more stable the in-plane position of the iron atom (and the smaller is the influence of protein globula and the *trans* ligand). In particular, it follows from Fig. 6 that the CO ligand produces a stronger crystal field than O_2. This explains in a natural way both the smaller influence of the steric hindrance of the *trans* ligand L_1 in the case of $Fe(P)(L_1)(CO)$ than in the case of $Fe(P)(L_1)(O_2)$ [128], and the weaker influence of the protein globula on the iron out-of-plane displacement in the hemoprotein CO complexes, than in the same complexes with O_2 [20,83,100,116,117,120].

The conclusion concerning the weak influence of the oxidation state of the iron atom on the magnitude of its out-of-plane displacement, in metalloporphyrin complexes with one axial ligand, remains valid for two axial ligands. This conclusion naturally explains why the heme geometry in cytochromes c and c-551 is almost completely independent of the iron oxidation state [122–126].

The problem of the influence of axial ligands on the magnitude of the iron atom out-of-plane displacement in metalloporphyrins was also investigated in refs. 71 and 129–131. In ref. 129 the influence of different factors on the iron geometry in complexes with one axial ligand is considered by calculation of the energy surface in the π-electron approximation combined with consideration of the σ interactions using empirical potential functions. It follows from this work that in the high spin complexes under consideration the metal out-of-plane displacement is determined mainly by the interaction of the metal atom with the porphyrin ring, modulated by the axial ligand, while the steric effects are less important.

Loew and Kirschner [130] performed a semiempirical (iterative extended Hückel) calculation of the potential energy curves for electronic states of different multiplicity as a function of the out-of-plane metal displacement in (Im)Fe(P) complexes. They showed that some special features of these curves for states of different multiplicity depend on the interelectronic interactions in the iron atom. The conclusion [71,131] that in ref. 130 the mixing of orbital spin states for $S = 2$ and $S = 1$ only is considered is unfounded, since the Hückel as well as other quantum-chemical calculations intrinsically include the mixing of different electronic states and among them also those of different parity. Therefore the statement of Mizuhashi [71,131] that the direct quantum-mechanical and pseudo-Jahn–Teller approaches are, in principle, different, cannot be accepted: both approaches consider the same interactions but in different ways. The Jahn–Teller approach separates the most important interactions revealing general laws which are less quantitative, but valid for different compounds; the direct quantum-chemical numerical calculations yield results which, although more quantitative, are valid only for the concrete compound for which the calculations were carried out.

In refs. 71 and 131 the adiabatic potential curves for states of different multiplicity are built up by a combination of the pseudo-Jahn–Teller mixing of the iron $3d$ and $4p$ states with the crystal field effect of the imidazole nitrogen atom. As emphasized in Section C, this approach, based on polarization effects only [77–79], ignores the most important covalent contribution to the pseudo-Jahn–Teller effect, the formation of additional covalent bonds between the metal atom and porphyrin ring by the out-of-plane displacement (Section B; see also ref. 129). Therefore the approach [77–79] cannot be correct even if the parameters can be chosen to satisfy the experimental data. (In the work reported in refs. 68–70 the vibronic reduction of the A_{2u} displacement, as mentioned above, is overestimated.)

The influence of vibronic effects on the geometry of the active centre of hemoglobin in the process of oxygenation was also considered in ref. 132. In this work it is assumed that a Jahn–Teller t_{2g}–e_g interaction (t–e problem, see ref. 1) in the excited state of oxyhemoglobin may promote weakening of the iron–oxygen bond and the metal out-of-plane displacement in the deoxy form. However, as shown in refs. 133 and 134, the active vibration considered in ref. 132 does not include the metal displacement and therefore it cannot be responsible for the changes in the prosthetic group of the hemoproteins under consideration.

(iii) Geometries of coordination of diatomics

It is known that diatomics are usually coordinated to metalloporphyrins in two modes: linearly (Fig. 7(a)) and bent (Figs. 7(b) and 7(c)) [13,14,94,135,136]; in some recent studies [14,84,94,137–139] a symmetric coordination (Fig. 7(d)) of oxygen is assumed. When included in the protein, the geometry of ligand coordination may be different from that observed in model compounds [20,98,100,116,117]. In this subsection, we consider the vibronic mechanisms responsible for different geometries for coordination of diatomic molecules to metalloporphyrins and hemoproteins [29(a),76,140].

First we shall consider linear coordination (Fig. 7(a)) and its possible instability due to the pseudo-Jahn–Teller effect with respect to normal displacements which distort the linear configuration toward the bent configuration (Fig. 7(b)). The porphyrin molecule with a linearly coordinated axial ligand has C_{4v} symmetry. (The influence of the *trans* ligand, if present, is neglected since it does not essentially change the C_{4v} symmetry [47].)

The bending displacement (Fig. 7(b)) in this point group transforms as the E representation. Therefore the vibronic constant of mixing of the ground state with an appropriate excited state is non-zero, if (and only if) the direct product of their representations contain the E representation. Since the lowest excited states are formed by one-electron excitation of the ground state, i.e. by an electron transfer from the populated MO to the empty (or partially filled) MO, the vibronic constant is non-zero if the direct product of the irreducible representations of these two MO contains the E representation.

In Fig. 8 is shown a qualitative one-electron MO energy scheme, based on quantum–chemical calculations, for complexes of metalloporphyrins with linearly coordinated diatomics CO, NO and O_2 [30,47,84,85]. There are several possible combinations of one degenerate and one non-degenerate (or degenerate) MO, for which the direct product of their representations contains the E representation. However, not all the formally possible

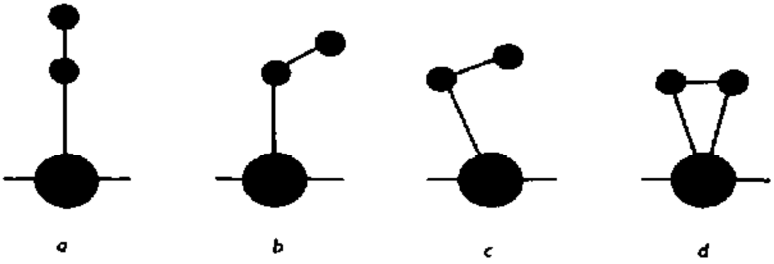

Fig. 7. Modes of coordination of diatomics to metalloporphyrins.

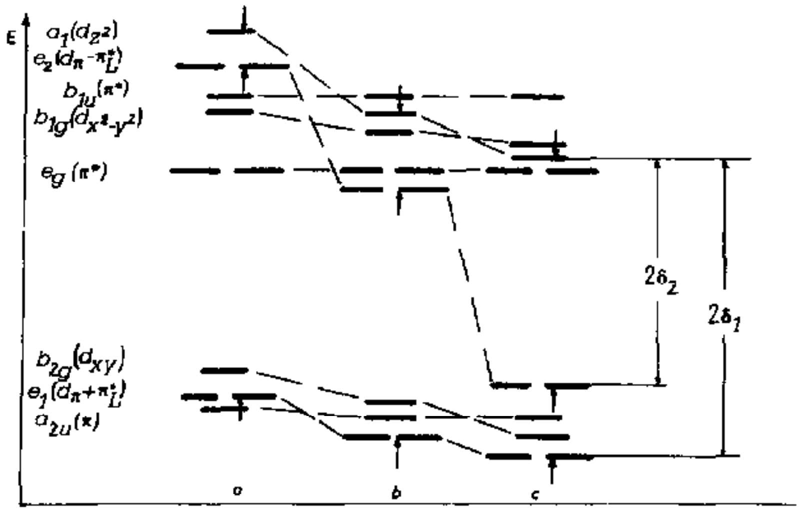

Fig. 8. Schematic MO energy diagram for linear end-on coordination of diatomics (a) CO, (b) NO and (c) O_2 with metalloporphyrins.

mixings are important to the vibronic effects: some of them may yield very small vibronic constants with a small contribution to the effect. The most important are those orbitals which contribute mostly to the metal–ligand bond [1]. Therefore in the case under consideration the vibronic mixing of one of the two e MOs, $e_1(d_\pi + \pi_L^*)$ or $e_2(d_\pi - \pi_L^*)$ (which are metal–ligand bonding and antibonding π orbitals respectively), with the metal $a_1(d_{z^2})$ orbital (which contributes predominantly to the metal–axial ligand σ bonding) is most essential. The appropriate energy gaps between these two mixing pairs of MOs are $2\delta_1$ and $2\delta_2$ respectively (Fig. 8). The contribution of the mixing of the porphyrin e MO and the metal orbitals $b_1(d_{x^2-y^2})$ and $b_2(d_{xy})$ (located in the plane of the porphyrin ring) with one another and with other MOs is negligible, since these orbitals do not take part directly in the bonding under consideration.

We shall consider first vibronic mixing of the ground $E(X, Y)$ state, e.g. for one electron in the e_2 MO, with one excited A_1 state by the E-type nuclear displacements, q_x and q_y, in the linear (with respect to q) approximation assuming that the high symmetry configuration corresponds to the point $q_x = q_y = 0$. The vibronic interaction operator in this case is [1,7]

$$V(r, q_x, q_y) = (\partial V/\partial q_x)_0 q_x + (\partial V/\partial q_y)_0 q_y \tag{38}$$

Using the Wigner–Eckart theorem (see refs. 7 and 81) we have

$$\langle X|(\partial V/\partial q_x)_0|A_1\rangle = \langle Y|(\partial V/\partial q_y)_0|A_1\rangle = \mathscr{F}$$

$$\langle Y|(\partial V/\partial q_x)_0|A_1\rangle = \langle X|(\partial V/\partial q_y)_0|A_1\rangle = 0 \tag{39}$$

and the appropriate secular equation for the energy levels of the E and A_1 states perturbed by the vibronic interactions is as follows:

$$\begin{vmatrix} -\delta-\mathscr{E} & 0 & \mathscr{F}q_x \\ 0 & -\delta-\mathscr{E} & \mathscr{F}q_y \\ \mathscr{F}q_x & \mathscr{F}q_y & \delta-\mathscr{E} \end{vmatrix} = 0 \tag{40}$$

where 2δ is the energy gap between the E and A_1 states at $q_x = q_y = 0$. In polar coordinates

$$q_x = \rho \cos\phi \quad q_y = \rho \sin\phi \tag{41}$$

and the roots of eqn. (39) are

$$\begin{aligned} \mathscr{E}_{1,3} &= \pm\left(\delta^2 + \mathscr{F}^2\rho^2\right)^{1/2} \\ \mathscr{E}_2 &= -\delta \end{aligned} \tag{42}$$

and for the lowest sheet of the adiabatic potential energy, also taking into account the elastic energy $(1/2)K_E\rho^2$, we obtain

$$E(\rho, \phi) = \tfrac{1}{2}K_E\rho^2 - \left(\delta^2 + \mathscr{F}^2\rho^2\right)^{1/2} = -\delta + \tfrac{1}{2}\left(K_E - \frac{\mathscr{F}^2}{\delta}\right)\rho^2 + \ldots \tag{43}$$

Equation (43) shows that the ground state force constant K_E becomes reduced by an amount $\mathscr{F}^2/\delta$, and if

$$(\mathscr{F}^2/\delta) > K_E \tag{44}$$

the ground state becomes unstable with respect to nuclear displacements of the E type, its adiabatic potential surface acquiring the shape of a circular trough. The condition of vibronic instability (eqn. (44)) can easily be generalized to the case of vibronic mixing of the ground E state with two excited A_1 states, $A_1^{(1)}$ and $A_1^{(2)}$, by the E displacements (cf. eqn. (7)):

$$\frac{\mathscr{F}_1^2}{\delta_1} + \frac{\mathscr{F}_2^2}{\delta_2} > K_E \tag{45}$$

where $\mathscr{F}_1$ and $\mathscr{F}_2$ are the linear vibronic constants of the appropriate two mixings, E with $A_1^{(1)}$ and E with $A_1^{(2)}$, their energy gaps being $2\delta_1$ and $2\delta_2$. In this case, too, the adiabatic potential surface is an axial trough (Fig. 9).

For the sake of simplicity we now pass to the more useful (although less rigorous) one-electron MO language in which the adiabatic potential energy can be presented as a sum of MO energies $\mathscr{E}_i(\rho, \phi)$ multiplied by the appropriate population numbers p_i:

$$E(\rho, \phi) = \tfrac{1}{2}K_E\rho^2 + \sum_i p_i\mathscr{E}_i(\rho, \phi) \tag{46}$$

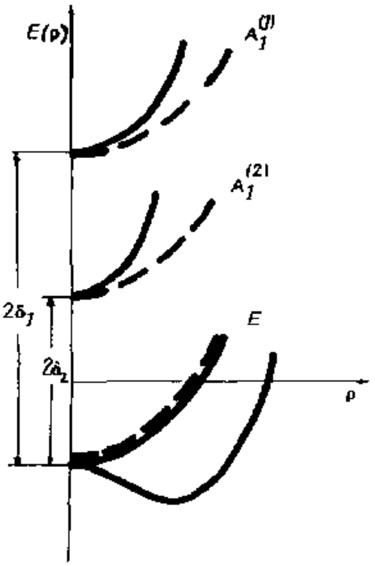

Fig. 9. Adiabatic potential curves for the terms $A_1^{(1)}$, $A_1^{(2)}$ and E with (solid curves) the without (broken curves) the pseudo-Jahn–Teller effect taken into account.

In this presentation the condition of instability (eqn. (45)) takes the following form:

$$\left[\mathscr{F}_1^2(p_1-p_3)/\delta_1\right]+\left[\mathscr{F}_2^2(p_2-p_3)/\delta_2\right]>K_E \tag{47}$$

where $\mathscr{F}_1$ and $\mathscr{F}_2$ are the linear vibronic constants of the vibronic mixings of the e_1 MO with the a_1 MO and the e_2 MO with a_1 MO respectively, and p_3, p_1 and p_2 are the population numbers of the orbitals a_1, e_1 and e_2 respectively.

Let us consider now how these vibronic effects influence the geometry in concrete cases of complexes of metalloporphyrins with CO, NO and O_2.

In the case of (CO)Me(P) the $2\delta_2$ and $2\delta_1$ values are of the order of magnitude of 0.3 eV and 4 eV respectively (Fig. 8(a)) [30,47,85]. Taking into account the orders of magnitude of the vibronic constants $\mathscr{F}_1$ and $\mathscr{F}_2$ and the force constant K_E, we can see that if only the e_1 MO is populated ($p_2=p_3=0$), the inequality (47) is not valid, since δ_1 is too great. Hence in this case the linear geometry is stable. If the e_2 MO is also populated ($p_1\neq 0$, $p_2\neq 0$, $p_3=0$), then condition (47) can be obeyed owing to the much larger additional contribution of the second term. In this case, obviously, the bent geometry of coordination is expected. However, in all the complexes of $3d^n$ metalloporphyrins with CO studied so far, the e_2 MO is not populated (in the ground state), and this explains the observed experimentally linear coordination of CO in (CO)Fe(P) and (CO)Co(P)

[50,94,141–144]. The calculations [47,85] show that in all the $3d^n$ complexes under consideration (including $3d^{10}$(Zn)) the e_2 orbital is not expected to be populated, and hence in all these complexes the linear coordination of CO (Fig. 8(a)) is expected.

The opposite situation emerges in the case of (O_2)Me(P). Here the two e MOs are at approximately the same energy separation from a_1 ($2\delta_2 \approx 2.5$ eV; $2\delta_1 \approx 3$ eV [47]) and almost equally contribute to the softening of the linear coordination. Therefore the linear coordination of O_2 is expected to be soft or even unstable for any number of metal d electrons. However, if this number exceeds four, the distortion may increase sharply since in this case both e-type MOs contribute to the vibronic softening. This qualitative conclusion agrees well with experimental data [13,14,90,136,145–151].

For (NO)Me(P) complexes with linear coordination of NO the $2\delta_1$ and $2\delta_2$ values are almost the same (of the same order of magnitude) as in the (CO)Me(P) complexes. However, the MO energy level ordering is different from that of (CO)Me(P) (Fig. 8(b)), and the e_2 MO becomes populated when the number of metal d electrons exceeds five. Therefore for complexes of NO with $3d^n$ metalloporphyrins linear coordination of NO is expected, if $n \leqslant 5$, and non-linear coordination is expected for $n > 5$. In the latter case the increase in the number of d electrons, increasing the population number p_2, increases the softening (bending angle) of the linear configuration (see eqns. (46) and (47)). In particular, in porphyrin complexes of iron(III) and manganese(II), linear coordination of NO is expected, whereas in iron(II) and cobalt(II) the bent configuration of coordinated NO is expected, the bending being greater in the case of cobalt(II) than in iron(II). All these conclusions are confirmed by experimental data [14,94,152–157].

It follows from eqn. (43) that the magnitude of distortion of the linear geometry ρ_0 is the greater, the less is the energy gap $2\delta_2$ between the MO $e_2(d_\pi - \pi_L^*)$ and $a_1(d_{z^2})$ and the greater is the vibronic constant $\mathscr{F}_2$. Therefore coordination of the second axial ligand, which increases the δ_2 value and reduces (by covalent effects) the $\mathscr{F}_2$ value, must reduce the bending of the NO coordination. This conclusion is also confirmed experimentally [94,153,154]. Moreover, following the shape of the E displacements, the coordination geometry in Fig. 7(c), and not Fig. 7(d), is expected in agreement with experimental data [149].

It follows from the above discussion that the vibronic approach allows not only the origin of all the experimental data on the coordination geometries of diatomics to metalloporphyrins to be explained, but also the possible geometries of coordination of small molecules in complexes not yet synthesized or studied to be predicted. In the case of metalloporphyrins with diatomics, the prediction is straightforward: for distortion of linear coordination it is necessary (and enough) to populate the $e_2(d_\pi - \pi_L^*)$MO.

So far we have employed an approximate vibronic theory linear in q_x and q_y. This generates an adiabatic potential surface having the form of an axial trough for which the bent configuration of the coordinated diatomics is independent of the angle ϕ (in the plane of the porphyrin ring) specifying the direction of bending. In this approximation the symmetry of the system increases from the initial C_{4v} to $C_{\infty v}$ (see the E–e problem in refs. 1, 6 and 7). To avoid this non-physical result the quadratic terms of the vibronic interactions should be taken into account. In so doing, the operator of the vibronic interactions, instead of eqn. (38), becomes

$$V(r, q_x, q_y) = (\partial V/\partial q_x)_0 q_x + (\partial V/\partial q_y)_0 q_y + \tfrac{1}{2}(\partial^2 V/\partial q_x^2)_0 q_x^2 + (\partial^2 V/\partial q_x \partial q_y)_0 q_x q_y + \tfrac{1}{2}(\partial^2 V/\partial q_y^2)_0 q_y^2 \tag{48}$$

Using the Wigner–Eckart theorem we obtain in the case of E–A_1 mixing the following equation:

$$\begin{vmatrix} -\delta + \beta(q_x^2 - q_y^2) - \mathscr{E} & 2\gamma q_x q_y & \mathscr{F} q_x \\ 2\gamma q_x q_y & -\delta - \beta(q_x^2 - q_y^2) - \mathscr{E} & \mathscr{F} q_y \\ \mathscr{F} q_x & \mathscr{F} q_y & \delta - \mathscr{E} \end{vmatrix} = 0 \tag{49}$$

where β and γ are the appropriate reduced matrix element–second-order vibronic constants [1]:

$$\beta = \tfrac{1}{2}\langle X|(\partial^2 V/\partial q_x^2)_0|X\rangle$$

$$\gamma = \tfrac{1}{2}\langle X|(\partial^2 V/\partial q_x \partial q_y)_0|Y\rangle$$

In polar coordinates (eqn. 41), eqn. (49) transforms to

$$\begin{aligned} &\mathscr{E}^3 + \delta\mathscr{E}^2 - \mathscr{E}\left[\delta^2 + \mathscr{F}^2\rho^2 + \rho^4(\beta^2 \cos^2 2\phi + \gamma^2 \sin^2 2\phi)\right] \\ &\quad - \delta^3 - \delta\mathscr{F}^2\rho^2 - (\beta \cos^2 2\phi + \gamma \sin^2 2\phi)\mathscr{F}^2\rho^4 \\ &\quad + \delta\rho^2(\beta^4 \cos^2 2\phi + \gamma^2 \sin^2 2\phi) = 0 \end{aligned} \tag{50}$$

The cubic eqn. (50) has three roots $\mathscr{E}_j$, the corresponding adiabatic potentials being as follows:

$$E_j(\rho, \phi) = \tfrac{1}{2}K_E\rho^2 + \mathscr{E}_j(\rho, \phi) \tag{51}$$

from which it follows that at the extrema points

$$\left(\frac{\partial E_j}{\partial \phi}\right)_0 = \left(\frac{\partial \mathscr{E}_j}{\partial \phi}\right)_0 = 0 \tag{52}$$

Taking the derivative of eqn. (50) over ϕ and using eqn. (52), we obtain

$$(\gamma-\beta)\left[(\mathscr{E}_{j0}-\delta)(\gamma+\beta)-\mathscr{F}^2\right]\sin 4\phi=0 \tag{53}$$

From this equation it is seen that if $\gamma\neq\beta$, the extrema points with respect to ϕ are determined by the equation

$$\sin 4\phi=0$$

with the roots

$$\phi=\tfrac{1}{4}m\pi \qquad (m=0,1,\ldots 7) \tag{54}$$

Four of these points are minima and the other four are maxima with respect to the angle ϕ. In order to specify the maxima and minima the Öpik and Pryce [158] procedure can be employed. One of the extremum coordinates is [76]

$$\phi=0$$

$$\begin{aligned}\rho=2\left[\beta^2K_E^2(K_E+\beta)\right]^{-1/2}&\Big\{|\mathscr{F}|(\beta+2K_E)K_E\\&\times\left[(\mathscr{F}^2-\delta\beta)K_E(K_E+\beta)\right]^{1/2}-K_E^2(K_E+\beta)(2\mathscr{F}^2-\delta\beta)\Big\}^{1/2}\end{aligned} \tag{55}$$

and its energy is

$$E_0=-2\beta^{-2}\left\{|\mathscr{F}|(K_E+\beta)^{1/2}-\left[(\mathscr{F}^2-\delta\beta)K_E\right]^{1/2}\right\}^2+\delta \tag{56}$$

With these expressions the condition of instability with respect to bending displacements ρ in the direction $\phi=0$ (from symmetry considerations the same is true for $\phi=\pi/2$, π, $3\pi/2$) at the point $\rho=\phi=0$ is

$$(\mathscr{F}^2/\delta)>K_E+\beta \tag{57}$$

The energy of the next (to $\phi=0$) extremum at the point

$$\phi=\pi/4$$

$$\begin{aligned}\rho=2\left[\gamma^2K_E(K_E+\gamma)\right]^{-1/2}&\Big\{|\mathscr{F}|(\gamma+2K_E)K_E\left[(\mathscr{F}^2-\delta\gamma)K_E\right.\\&\left.\times(K_E+\gamma)\right]^{1/2}-K_E^2(K_E+\gamma)(2\mathscr{F}^2-\delta\gamma)\Big\}^{1/2}\end{aligned} \tag{58}$$

is as follows:

$$E_{\pi/4}=-2\gamma^{-2}\left\{|\mathscr{F}|(K_E+\gamma)^{1/2}-\left[(\mathscr{F}^2-\delta\gamma)K_E\right]^{1/2}\right\}^2+\delta \tag{59}$$

while the condition of instability at $\rho=\phi=0$ for $\phi=\pi/4$ (and hence for $\phi=3\pi/4$, $5\pi/4$, $7\pi/4$) is

$$(\mathscr{F}^2/\delta)>K_E+\gamma \tag{60}$$

It can easily be seen from eqns. (56) and (59) that E_0 and $E_{\pi/4}$ are monotonic functions of β and γ respectively, and therefore if

$$\beta > \gamma \tag{61}$$

then the energy minimum corresponds to the ρ coordinate determined by eqn. (58) and to the ϕ coordinates as follows:

$$\phi = \tfrac{1}{4} m\pi \qquad (m = 1, 3, 5, 7) \tag{62}$$

whereas the points with the ρ coordinate according to eqn. (55) and

$$\phi = \tfrac{1}{4} m\pi \qquad (m = 0, 2, 4, 6) \tag{63}$$

are saddle points. However, if

$$\beta < \gamma \tag{64}$$

then the points given by eqns. (55) and (63) are minima, whereas those with the coordinates given by eqns. (58) and (62) are saddle points. It is obvious that, depending on the barrier height between the minima, there is a smaller or greater probability of the ligand moving between the minima (to rotate around the axial axes). Both conclusions about the direction of bending and of possible ligand rotation are confirmed experimentally [94,146–149,152, 154,155,159,160]. Thus the vibronic approach incorporating quadratic vibronic terms also explains the bending direction and possible rotations of the bent configuration.

The instability of the linear coordination may result in either the bent (Figs. 7(b) and 7(c)) or the symmetric (Fig. 7(d)) configuration. In order to distinguish between these two possibilities the symmetric configuration can be tested for vibronic instability with respect to distortion toward the bent configuration. The procedure is similar to that performed above, and is illustrated below with the example of oxygen coordination. In the symmetric configuration (Fig. 7(d)) the system possesses C_{2v} symmetry, while the normal displacements of ligand bending transform as the B_1 or B_2 representations of this group. Under these displacements the vibronic contribution to the softening of the symmetric configuration involves mixing of either the $b_1(d_{xz})$ MO or the $b_2(d_{yz})$ MO with $a_1(d_{z^2})$ orbital. Since both the mixing orbitals are non degenerate, the vibronic pseudo-Jahn–Teller problem is reduced to the solution of eqn. (2). According to the results of refs. 84 and 137, this interaction is much weaker in the complex (O_2)Mn(P) than in (O_2)Fe(P) where the oxygen molecule is bent [90,94,146]. Therefore we can assume that in (O_2)Mn(P) in contrast with (O_2)Fe(P), symmetric coordination of oxygen is possible [14,94,138,139].

The inclusion of a metalloporphyrin complex into a crystal lattice or into a protein may result in a change in ligand geometry, firstly owing to steric hindrance [15,20,98,114–117,135,159–166]. As shown in these studies, steric effects may lead either to distortion of linear coordination in proteins, as compared with the model compounds, or to discrimination of the equivalent configurations at the points given by eqns. (62) and (63) resulting in localization of the system near one of the minima (or even in a change in its coordinates).

The problem of coordination geometry of diatomics is discussed in a series of papers [141,167–177]. The researchers [141,167,168] suggest a qualitative model for the interaction of the metalloporphyrin and ligand MO, in which the energetic preference of the bent coordination is explained by the hybridization of the π and σ orbitals. The importance of such hybridizations is confirmed in refs. 169 and 170. In refs. 84, 137 and 171–176 the coordination geometry is investigated by means of direct quantum-chemical calculation. In ref. 177 the mechanism determining the coordination geometry of diatomics (in particular, NO) is considered by including the vibronic interactions. However, in contrast with the studies described in refs. 29(a), 76 and 140, the researchers [177] consider an interaction with the non degenerate displacement, which in fact describes the distortion of the porphyrin ring, but not the ligand geometry.

Several papers are devoted to investigations of the Jahn–Teller effect in the ground electronic state of some hemoproteins [178–183]. The anisotropic part of the g factor of ferrihemoglobin complexes with azide is attributed to the combined influence of the Jahn–Teller effect, rhombicity and covalency [178,179]. The temperature dependence of the magnetic susceptibility and of the quadrupole splitting of deoxyhemoglobin is also interpreted in the framework of the Jahn–Teller effect [181–183]. (However, it should be noted that according to refs. 184–186, for a correct description of the experimental data from Mössbauer spectroscopy, the low symmetry components of the crystal field within the protein molecule must be taken into account.) A vibronic approach to the study of proton dynamics in free base porphyrins is given in ref. 186(a).

E. PHOTOLYSIS OF COMPLEXES WITH DIATOMICS

The nature of the mutual influence of the active centre and globula in hemoproteins has been subject to intensive investigation by means of flash photolysis [23,187–193] used in combination with light absorption [189,194–207], resonance Raman spectroscopy [193,208–214], natural dichroism [192], magnetic circular dichroism [206,215,216], IR [201,217] and Mössbauer spectroscopy [218], extended X-ray absorption fine structure (EXAFS) [219,220] and magnetic susceptibility [221].

The method of flash photolysis consists of the photodissociation of the model complex or the hemoprotein complex into the ligand and protein, followed by investigation of the relaxation effects in the heme and different parts of the protein globula. Using this method, the mechanism of coordination of diatomics to myoglobin, hemoglobin and its separate chains [197–201,203,207], cytochrome P-450 and its models [194,206,215,216], peroxidase [189], as well as the dynamics of the protein globula [193,202,206–210,214,216–218] and the nature of protein movement in the membrane [192] etc., were considered.

In this section the mechanism of photolysis of complexes of 3*d* metalloporphyrins and hemoproteins with diatomics is investigated by the vibronic approach in which the vibronic interactions in the excited states of these systems are considered.

(i) Formulation of the problem

The photolysis of diatomic (L) complexes with metalloporphyrins and hemoproteins has been studied experimentally by many groups [195,196, 202–205,208–213,218–220,235,237,239]. The following conclusions can be reached.

(a) The complexes of 3*d* Me(P) with linearly coordinated ligands $(L)^l$Me(P) and appropriate hemoproteins $(L)^l$HP dissociate with a quantum yield of $\phi(L)^l \approx 0.5$–1.0 [195,196,204,224–229], whereas for complexes of Me(P) with bent coordinated ligands $(L)^b$Me(P) and appropriate hemoproteins $(L)^b$HP the quantum yield is much smaller, $\phi(L)^b \approx 10^{-2}$–$10^{-4}$ [195,196,204,222,225,226,228,230–233], the complex $(NO)^b$Co(TPP) with $\phi(NO)^b \approx 1$ being the only known exception [238].

(b) The low $\phi(O_2)^b$ values have been related to fast geminate recombination [231,236]. However, experimental data [226,228,232] show that geminate recombination can reduce the quantum yield of photodecay at most by a factor of two. Therefore it is suggested [222,226,228,232,234] that the low $\phi(O_2)^b$ values must be attributed to more efficient radiationless relaxations to non-dissociative states in the oxygen complexes, than in complexes with carbon monoxide. It has been shown recently [319] that the geminate recombination is absent at least in the first 10 ps. In ref. 233 the low $\phi(NO)^b$ value is related to geminate recombination, although the possibility of radiationless relaxation to non dissociative states is not excluded.

(c) The characteristic photodissociation time is $\tau \approx 10^{-13}$–10^{-12} s [210, 222–224,227–229,231–233].

(d) The photodecay quantum yield for the (L)Me(P) and (L)HP complexes is slightly sensitive to the frequency of the absorbed light in the region 280–620 nm [204,224,228].

In spite of intensive experimental investigation, the photolysis mechanism relevant here remained unclear for a long time. The following four questions are of primary interest in the determination of the photolysis mechanism.

(1) Can the main features of the photolysis be explained in terms of direct decay of the photoexcited state, or are radiationless relaxation processes essential?

(2) What is the origin of the electronic state responsible for the photodecay?

(3) What is the coordinate of photodecay?

(4) In what state do the products of photodecay occur?

Let us discuss these questions in turn.

(1) If the characteristics of photolysis are determined predominantly by radiationless relaxations, then these can increase or reduce the magnitude of the quantum yield, depending on whether a dissociative or a non-dissociative term is populated by the radiationless transitions. In the former case, the quantum yield of bent complexes $(L)^{b}Me(P)$ and $(L)^{b}HP$ is expected to be at least but not less than that for linear $(L)^{l}Me(P)$ and $(L)^{l}HP$. Indeed, the radiationless transitions are expected to be more effective in the case of bent complexes owing to their lower symmetry causing more favourable conditions for selection rules. For radiationless transitions to a non dissociative state this reason may, in principle, explain the higher quantum yield of linear configurations, as compared with bent complexes, owing to the lower rate of transition to the non-dissociative state (and hence the higher probability of decay). However, this assumption seems unrealistic. Indeed, the formation of non dissociative terms (and transitions to and from them) depends critically on the details of electronic structure, and therefore it is extremely improbable that these electronic features remain the same in many different complexes $(CO)^{l}Fe^{II}(P)$, $(NO)^{l}Mn^{II}(P)$, $(NO)^{b}Co^{II}P$, and $(NO)^{l}Fe^{III}(P)$, yet change sharply when passing to $(NO)^{b}Fe^{II}(P)$, $(O_2)^{b}Fe^{II}(P)$ and $(O_2)^{b}Co^{II}(P)$.

However, the assumption of decay directly from the photoexcited state is not consistent with the weak dependence of the quantum yield on the frequency of absorbed light.

(2) To our knowledge the first discussion of the nature of the state responsible for photolysis was given for $(CO)^{l}Fe(P)$ [30]. On the basis of electronic structure calculations, it was assumed that the photodecay takes place owing to either the direct optical excitation $e(d_\pi + \pi_L^*) \rightarrow a_1(d_{z^2})$, or the relaxation of the optically excited state to that obtained by such excitation. However, in complexes with O_2 and linearly coordinated CO the above excited state is much higher in energy [47,85,240–243], than the state Q, the transition to which results in photodecay. Therefore the state $e(d_\pi + \pi_L^*) \rightarrow a_1(d_{z^2})$ cannot be responsible for photodecay in these complexes. However, the investigation of the dependence of the energy gap between the

ground and some excited states on the iron–ligand distance and on the angle of ligand bending [241–243] shows that bending of the linear coordination of CO leads to a sharp decrease in the energy of the $e(d_{\pi}+\pi_{L}^{*}) \rightarrow a_1(d_{z^2})$ state. Thus, as a result of the CO bending, this energy becomes equal or even lower than the optically populated Q state. On the basis of this result the researchers [241–243] concluded that for efficient photodecay a bent CO coordination is needed. This requirement is inconsistent with X-ray measurements [94,143,144] which show that in the complexes under consideration the CO ligand is linearly coordinated.

An alternative photolysis mechanism is suggested in refs. 204 and 244 where it is assumed that photodecay takes place directly from the singlet states $^1(\pi \rightarrow \pi^*)$ or their lower-in-energy triplet analogues $^3(\pi \rightarrow \pi^*)$ formed by light absorption within the Q and B bands. This assumption also explains the fact that the quantum yield does not depend on the frequency of absorbed light in the 280–620 nm region, but it disagrees with calculations [241–243]. However, the conclusion drawn from these calculations that the term under consideration is non dissociative cannot be considered as final. The conclusion is based on the result that the iron electronic environment remains almost unchanged by the above excitation, which is in disagreement with some other theoretical [240] and experimental [245–247] studies. Moreover, it is shown [240] that for a correct determination of the parameters of the Q and B states, higher order configurational interactions, up to the triple excited states, have to be taken into account, whereas in refs. 241–243 only single excited states were considered.

(3) It is assumed that the dissociation of the complex takes place along the totally symmetric coordinate, i.e. the metal–ligand bond breaks by elongation in the direction perpendicular to the plane of the porphyrin ring [30,47,85,241–243]. In this case photolysis may take place as a result of either direct population of the strong metal–ligand antibonding MO by photoexcitation, or as a result of mixing (by totally symmetric displacements) of the photoexcited state with the upper states containing antibonding orbitals. Unfortunately, calculations [241–243] do not contain data on the excited state energy dependence of the iron–ligand distance, and we cannot decide upon the nature of the decay of the $e(d_{\pi}+\pi_{L}^{*}) \rightarrow a_1(d_{z^2})$ state along the totally symmetric coordinate.Moreover, doubt is cast on this possibility by results [85] which show that all the electronic states obtained by one-electron excitation from the different metal–ligand MO to the most antibonding $a_1(d_{z^2})$ MO are bonding with respect to ligand displacement in the direction perpendicular to the porphyrin ring. Therefore a transition to these states cannot cause this mode of decay in the totally symmetric direction.

However, it is known that decay has to take place in the direction of the lowest potential barrier. At the top of the barrier the system is dynamically unstable, and since the vibronic mixing of the electronic state under consideration with the upper states is the only source of dynamic instability (see Section B and refs. 1 and 8–10), the direction and magnitude of this barrier is controlled by vibronic effects. In particular, the direction of the lowest barrier is expected to be that of strongest vibronic mixing with excited states [1,8–10,12,248].

Thus, if the photoexcited state is not dissociative, then the decay coordinate has to both increase the metal–ligand distance and strongly mix this state with close-in-energy higher states. In our case the only non totally symmetric coordinate containing the departure of the ligand is the E coordinate [167]. This coordinate also provides strong mixing of the photoexcited e MO (see below) with the upper MO, obtained by excitation from the e MO to the $a_1(d_{z^2})$ MO (see Section D). Note that this E coordinate, as shown in the previous section, is responsible for the distortion of the linear to the bent coordination in complexes of Me(P) with NO and O_2. As shown below in this section, this fact alone explains the origin of the essential difference in quantum yields of photolysis for linearly and bent coordinated complexes.

(4) As emphasized in part (3), the researchers in all previous work assumed that the photolysis of metalloporphyrin and hemoprotein complexes with diatomics takes place along the totally symmetric coordinate. With this assumption, the electronic structure of the photolysis products were studied in order to reveal the process scheme. In the mechanism of photolysis suggested within the vibronic approach, one of the main ideas is that the decay coordinate is the E coordinate, quite different from that assumed earlier. In this sense, investigation of the vibrational and rotational states of the products (which are more sensitive to the adiabatic potential shape along the dissociation path) is expected to give more information than the electronic states about the mechanism of photolysis.

Therefore the main problem in the elucidation of the photolysis mechanism is the determination of the coordinate of photodecay, which is directly related to the adiabatic potential surface of the photoexcited state. Below in this section, the vibronic approach is employed [249,250] to confirm the assumption that photodecay takes place along the E coordinate, to explain qualitatively the origin of the essentially different quantum yields in the linear and bent cases, and to suggest some experiments which can verify the proposed photolysis mechanism.

(ii) Influence of vibronic effects on the magnitude of the activation barrier to photodecay

We assume that photodecay of Me(P) and HP complexes with diatomics takes place directly from the photoexcited state (as shown in the next subsection, this condition is not absolutely necessary for consistency with the suggested photodecay mechanism) and we consider the adiabatic potential shape for this state. As shown by experiments on the absorption of polarized light [47,251], the photoexcited state is formed by electron excitation from the non-degenerate MO of the ground state to the *e*-type MO. Moreover, it follows from resonance Raman spectroscopy investigations on (L)HP complexes [245–247] that by this excitation the electronic structure of the iron site changes mainly by a change in the population numbers of its $e(d_\pi)$ orbitals. This was shown [240] to result from either covalency or the configuration interaction admixture of the metal–porphyrin MO to the pure porphyrin MO involved in the transitions $\pi \rightarrow \pi^*$. On the basis of these data we assume that the optically populated state ψ_1 has a contribution from the $e(d_\pi - \pi_L^*)$ MO. The next state obtained from ψ_1 by a one-electron excitation, $e(d_\pi - \pi_L^*) \rightarrow a_1(d_{z^2})$, is denoted by ψ_2, the energy gap between them being 2δ (the energy is read off from the middle of this interval). One of these two states (say ψ_1) is two-fold degenerate and the other (ψ_2) is non-degenerate, and therefore they mix under the *E*-type nuclear displacement. Without this vibronic mixing the adiabatic surfaces E_1 and E_2 of the states ψ_1 and ψ_2 in the space of the q_x and q_y components of the *E* displacement are as follows:

$$\begin{aligned} E_1(q_x, q_y) &= -\delta + \tfrac{1}{2}K_1\left(q_x^2 + q_y^2\right) \\ E_2(q_x, q_y) &= \delta + \tfrac{1}{2}K_2\left(q_x^2 + q_y^2\right) \end{aligned} \tag{65}$$

where K_i is the *E*-type force constant of the system in the state ψ_i.

If $K_1 > 0$ the state ψ_1 is stable. The decay may take place directly from this state only if there is another dissociative state, its adiabatic potential E_3 crossing E_1 (Fig. 10). Two limiting cases for the crossing are possible, i.e. with weak and strong interaction at the crossing points. In the case of weak interaction (corresponding to predissociation from the ψ_1 state) its influence on the shape of the crossing surfaces can be neglected, although it causes transitions between these states. In this case the height of the activation barrier to decay equals the energy difference between the crossing point and the minimum of the ψ_1 state. In the case of predissociation a high quantum yield of photolysis is not expected. Apparently, the observed (L)Me(P) and (L)HP photolysis is appropriate to the other limit when the interaction between the crossing states is strong.

Leaving apart the absolute value of the barrier height, we shall consider its reduction by vibronic mixing of the E_1 and E_2 states, assuming that this mixing does not essentially affect the interaction of E_1 with E_3. Without defining the nature of the E_3 term (it follows from refs. 241–243 that it may

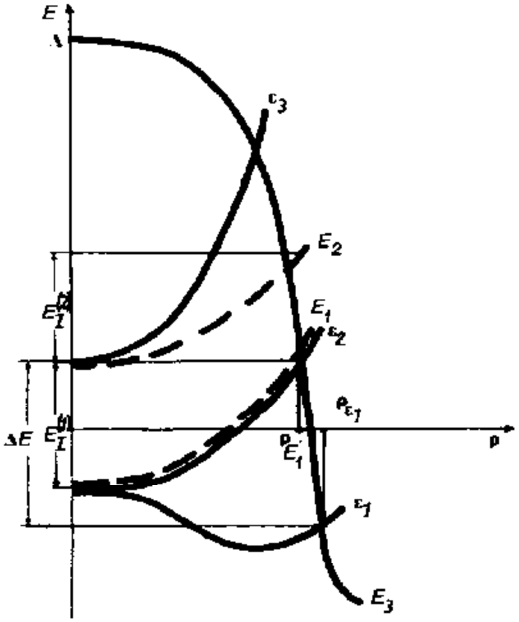

Fig. 10. The intersection of the decay term E_3 with the terms of the bound ψ_1 and ψ_2 states with (solid lines, $\mathscr{E}_1$, $\mathscr{E}_2$ and $\mathscr{E}_3$ terms) and without (broken lines, E_1 and E_2 terms) the vibronic mixing of these states by the E-type displacements taken into account.

be the $e(d_\pi + \pi_L^*) \rightarrow a_1(d_{z^2})$ state), we assume only that it crosses the E_1 state in the region of small enough q_x and q_y values, resulting in an activation barrier in this region. Therefore keeping only quadratic terms in the expansion of E_3 with respect to q_x and q_y, we have

$$E_3 = E_0 - \tfrac{1}{2}K_3\left(q_x^2 + q_y^2\right) \tag{66}$$

Consider now the influence of the vibronic mixing of the ψ_1 and ψ_2 states on the shape of the E_1 surface and hence on the activation barrier of decay from this state. In the linear approximation the vibronic interaction operator is given by eqn. (38) and, using the Wigner–Eckart theorem (eqn. (39)), we obtain, similarly to eqn. (40), the following secular equation where $\mathscr{F}_0$ is the constant of vibronic interaction with the E displacement:

$$\begin{vmatrix} E_1(q_x, q_y) - \mathscr{E} & 0 & \mathscr{F}_0 q_x \\ 0 & E_1(q_x, q_y) - \mathscr{E} & \mathscr{F}_0 q_y \\ \mathscr{F}_0 q_x & \mathscr{F}_0 q_y & E_2(q_x, q_y) - \mathscr{E} \end{vmatrix} = 0 \tag{67}$$

The roots of this equation, $\mathscr{E}_1$, $\mathscr{E}_2$ and $\mathscr{E}_3$, are the appropriate sheets of the adiabatic potential taking account of the vibronic mixing. In polar coordinates (eqn. (41)) we have

$$\mathscr{E}_2(\rho, \phi) = E_1(\rho, \phi)$$

$$\mathscr{E}_{1,3}(\rho, \phi) = \frac{E_1(\rho, \phi) + E_2(\rho, \phi)}{2} \pm \left\{\left[\frac{E_2(\rho, \phi) - E_1(\rho, \phi)}{2}\right]^2 + \mathscr{F}_0^2\rho^2\right\}^{1/2} \tag{68}$$

or, taking into account eqn. (65), we have

$$\mathscr{E}_{1,3}(\rho) = \frac{K_1 + K_4}{4}\rho^2 \pm \left[\left(\delta + \frac{K_2 - K_1}{2}\rho^2\right)^2 + \mathscr{F}_0^2\rho^2\right]^{1/2}$$

$$\mathscr{E}_2(\rho) = -\delta + \tfrac{1}{2}K_1\rho^2 \tag{69}$$

Thus the point of intersection of the $\mathscr{E}_1$ and E_3 terms is reduced by ΔE through the vibronic mixing (Fig. 10):

$$\begin{aligned}\Delta E = K_3\left[(K_1 + K_3)(K_2 + K_3)\right]^{-1}\Big(\Big\{\big[K_2(E_0 + \delta) \\ + K_1(\delta - E_0) + 2K_3\,\delta\big]^2 + 8\mathscr{F}_0^2\big[2\mathscr{F}_0^2 + K_1(E_0 - \delta) + 2K_3E_0 \\ + K_2(E_0 + \delta)\big]\Big\}^{1/2} - \big[K_2(E_0 + \delta) + K_1(\delta - E_0) + 2K_3\,\delta\big]\Big)\end{aligned} \tag{70}$$

For any value of $\mathscr{F}_0 \neq 0$, $\Delta E > 0$, and the greater the value of $\mathscr{F}_0$, the larger is ΔE. Assuming, as mentioned above, that the terms E_1 and $\mathscr{E}_1$ (Fig. 10) interact almost equally with the term E_3, we may state that the pseudo-Jahn–Teller (vibronic) mixing lowers the activation barrier by the same value ΔE.

For some simplification of the above formulae, we assume that K_3 is large enough, while ΔE is relatively small, so that if the difference between ρ coordinates of the intersection of the terms $\mathscr{E}_1$ and E_1 with E_3 is small enough (Fig. 10), we can assume the approximation

$$\rho_{E_1} \approx \rho_{\mathscr{E}_1} = \rho_0 \tag{71}$$

In this approximation the energy at the point of intersection between E_1 and E_3 is

$$E_1 = -\delta + \tfrac{1}{2}K_1\rho_0^2 \tag{72}$$

The vibronic interaction lowers this energy, and hence the activation barrier, by

$$\Delta E_A = \left[\left(\delta + \frac{K_2 - K_1}{4}\rho_0^2\right)^2 + \mathscr{F}_0^2\rho_0^2\right]^{1/2} - \left(\delta + \frac{K_2 - K_1}{4}\rho_0^2\right) \tag{73}$$

It is seen from this equation that the smaller the value of K_2, i.e. the larger the contribution of the antibonding MO to the vibronically admixed ψ_2 state, the greater is ΔE_{A}. Denoting $\mathscr{F}_0^2/K_1 = E_{\mathrm{JT}}^{(1)}$, $K_1\rho^2/2 = E_{\mathrm{I}}^{(1)}$ and $K_2\rho_0^2/2 = E_{\mathrm{I}}^{(2)}$ we can obtain, instead of eqn. (73), the following expression:

$$\Delta E_{\mathrm{A}} = \left\{\left[\delta + \frac{E_{\mathrm{I}}^{(2)} - E_{\mathrm{I}}^{(1)}}{2}\right]^2 + 2E_{\mathrm{JT}}^{(1)}E_{\mathrm{I}}^{(1)}\right\}^{1/2} - \left[\delta + \frac{E_{\mathrm{I}}^{(2)} - E_{\mathrm{I}}^{(1)}}{2}\right] \tag{74}$$

(iii) Mechanism of photolysis

Considering the adiabatic surface of the lowest sheet of the photoexcited state $\mathscr{E}_1$ obtained above, we can separate the following possible qualitatively different variants for the properties of the system discussed in Section E (ii).

If $E_{\mathrm{JT}}^{(1)} < \delta$, then linear coordination of the diatomics in the photoexcited state ψ_1 is stable, although, as seen from eqn. (69), it has an elasticity constant softened by the amount $\mathscr{F}_0^2/\delta$. However, as shown in the previous section, in the systems under consideration, the population of the $e(d_\pi - \pi_{\mathrm{L}}^*)$ MO results in an opposite inequality, $E_{\mathrm{JT}}^{(1)} > \delta$, the linearly coordinated configuration being unstable. If, in addition the inequality $\Delta E_{\mathrm{A}} < E_{\mathrm{A}}$ (E_{A} is the activation energy for the dissociation of the state in the absence of vibronic mixing (Fig. 11(a)) is obeyed, the point of the top of the barrier is higher than that at $\rho = 0$ (Fig. 11(b)). In this case the ψ_1 state is bonding, provided it is generated at $\rho < \rho_0$ (ρ_0 is the point of intersection).

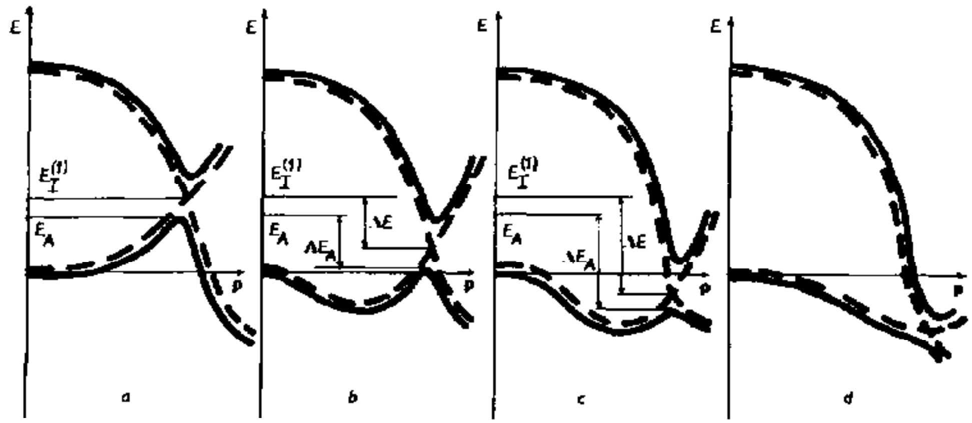

Fig. 11. The cross-section of the lowest adiabatic potential surface along the E coordinate without (a), and with weak $\Delta E_{\mathrm{A}} < E_{\mathrm{A}}$ (b), sufficiently strong $\Delta E_{\mathrm{A}} > E_{\mathrm{A}}$ (c), and very strong (d) pseudo-Jahn–Teller effect in the cases of weak (broken curves) and strong (solid curves) interaction with the decay term E_3.

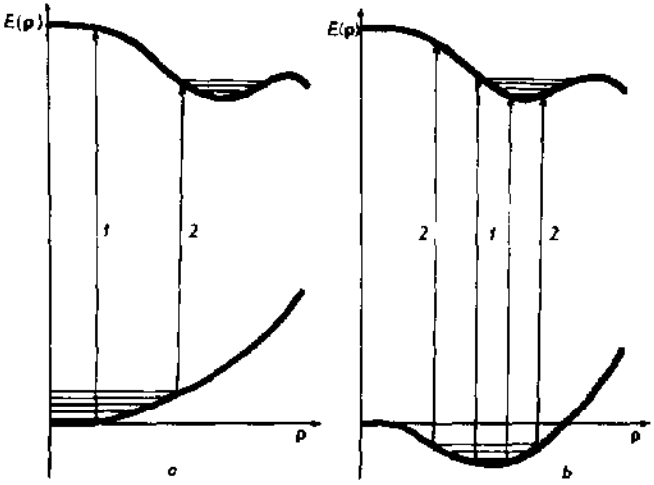

Fig. 12. Possible types of photoexcitation of (a) $(L)^1Me(P)$ and (b) $(L)^bMe(P)$ at low (line 1) and high (line 2) temperatures.

For $\Delta E_A > E_A$, either the barrier top point is lower in energy than that at $\rho = 0$ (Fig. 11(c)), or the adiabatic curve decreases monotonically (Fig. 11(d)). In the former case the system in the ψ_1 state generated at $\rho = 0$ occurs in the continuous spectrum with respect to the E displacements and decays, whereas if generated at the minimum point (Fig. 11(c)), it is stable. Independently of the mode of generation of the photoexcited state, the case of Fig. 11(d) is appropriate to a dissociative situation.

Let us consider now the qualitatively different situations which occur by photoexcitation to the ψ_1 state of two different classes of complexes: (a) linearly coordinated $(L)^1Me(P)$, and (b) bent coordinated $(L)^bMe(P)$. In the case (a), as seen from Fig. 12(a) after the Franck–Condon electronic transition, the system falls at a point near to $\rho = 0$, which in the case of a strong pseudo-Jahn–Teller effect ($\Delta E_A > E_A$) in this state corresponds to the continuous spectrum. This results in the decay of the system along the E coordinate (Fig. 12(a)).

Another situation occurs in the case (b). As shown in Section D, the vibronic effects responsible for ligand bending are due to the mixing of the populated $e(d_\pi - \pi_L^*)$ MO with the empty $a_1(d_{z^2})$ MO. Therefore the addition of one electron to the $e(d_\pi - \pi_L^*)$ MO does not essentially change the adiabatic potential shape (cf. the geometries of $(NO)^bFe(P)$ and $(NO)^bCo(P)$ [14]). This means that after the electronic transition by light absorption, shown in Fig. 12(b) the system occurs at a point near the minimum of the adiabatic surface corresponding to the bonded state, for which dissociation may only take place when the higher vibrational states are populated. In this case the low photodissociation quantum yield occurs as a result of competition between the low probability of population of high vibrational states (determined by the height of the potential barrier) and fast ($\tau \leqslant 10^{-12}$ s [252–256]) radiationless relaxations.

The same is true when the dissociation state under consideration (primarily involving the $e(d_\pi - \pi_L^*)$ MO) is generated as a result of a radiationless transition from another optically excited state, provided the system does not fall into strongly excited vibrational E states as a result of this transition. Under this condition the system occurs at a point near $\rho = 0$ of the state and behaves as described above.

(iv) Discussion of results

The photolysis mechanism revealed above for (L)Me(P) complexes answers the questions in Section E (i).

(1) It is most probable that photodecay takes place directly from the optically excited states which interact strongly with the dissociative term. As a result of this interaction the system in the process of decay moves along the adiabatic potential surface in the direction of the E (bending) displacement. In the absence of an activation barrier in this direction the process of photodecay is highly efficient ($\phi \approx 1$). In the opposite case of a high barrier, the decay efficiency is determined by competition between the probability to overcome the barrier and the probability for radiationless transitions to non-dissociative states.

(2) The optically excited Q and B states have a contribution from the $e(d_\pi - \pi_L^*)$ MO owing to covalency and/or configurational interaction (the role of the $e(d_\pi - \pi_L^*)$ MO in ligand bonding and the photolysis of Me(P) complexes is also discussed in ref. 257).

(3) Photodecay takes place along the E coordinate. In the optically populated states the linear coordination of the ligand is unstable with respect to bending which is just the same E coordinate. The bending of the ligand in the photoexcited state results in its intersection with the dissociative term E_3 (which can be obtained from the ground state by an electron $e(d_\pi + \pi_L^*) \rightarrow a_1(d_{z^2})$ excitation [241–243]). The interaction between the photoexcited state and the dissociative state realizes the situation described above in part (1), with additional emphasis that in the elucidation of the peculiarities of photolysis, the shape of the cross-section of the adiabatic potential surfaces of the interacting states along the E coordinate is most important.

(4) As seen from Fig. A1 of ref. 167, the normal E coordinate is a symmetrized displacement containing a superposition of the rotation of the ligand and its shift as a whole parallel to the porphyrin ring (overall

appearing as a bending). Therefore immediately after photodecay the population of the rotational states of the free ligand will be thermodynamically non-equilibrated. (In this sense the photolysis of (L)Me(P) resembles the photodissociation of ICN → I + CN [258–263], in which the CN molecule after dissociation occurs in inversely populated rotational states.) According to Fig. 12, the CO molecule has to emerge from the photodecay in a fast rotating state. This conclusion is in indirect agreement with data [201] concerning the rotation of the CO molecule by recombination at low (about 40 K) temperatures. As already mentioned above, in the vibronic photolysis mechanism under consideration, the high quantum yield for $(L)^1Me(P)$ is due to photoexcitation to the state which falls in the continuous spectrum with respect to E displacements (Fig. 12(a)). The low quantum yield for bent complexes, $\phi(L)^b \approx 10^{-2}$–$10^{-4}$, is due to the metastable photoexcited state (Fig. 12(b)). This conclusion is in good agreement with results [222] showing that the complex $(O_2)^bHb$, compared with $(CO)^1Hb$, has a higher lifetime in the excited state, and relaxes to the ground state without decay.

The metastable state can only be realized if the adiabatic potential surface has the shape shown in Figs. 11(b) and 11(c), i.e. the photoexcited state has a stable bent configuration. If this state is strongly unstable with respect to bending and has no minima in the E direction (Fig. 11(d)), then high photolysis quantum yields are also expected in complexes $(L)^bMe(P)$ with bent configurations. Apparently, this is the situation which occurs in $Co(TPP)(NO)^b$ and $Co(OEP)\ (NO)^b$ [238].

It also follows from this development that for high quantum yields in the cases of $(CO)^1Me(P)$ and $(CO)^1HP$, distortion of linear coordination in the ground state is not necessary (contrary to the statement of refs. 241 and 243); the bending takes place in the excited state. This result also confirms the assumption [204] concerning the rearrangement of the nuclear subsystem in the excited Q state leading to a reduction in energy of the $e(d_\pi + \pi_L^*) \rightarrow a_1(d_{z^2})$ state.

So far we have considered vibronic effects in the photolysis of complexes of metalloporphyrins with diatomics. In order to apply these results to appropriate hemoprotein complexes the influence of the protein on the active centre must be taken into account. If this influence is small, the expected quantum yields, $\phi(L)$, are almost the same for both (L)MeP and (L)HP. In the opposite case of a strong influence of the protein upon the adiabatic potential shape in the E direction, the $\phi(L)$ values may differ significantly. Therefore some conclusions about the coordination geometry of diatomics in proteins can be drawn from the observed $\phi(L)$ values.

For instance, X-ray data show [29] that in the crystalline state the coordination of CO in (CO)Mb is strongly non-linear (bent). However, the photolysis quantum yield of (CO)Mb in solution is very high, $\phi(CO) \approx 0.7$

[204,225,230,264,265]. This testifies to the conclusion of refs. 264 and 266 that there is almost linear coordination of CO in (CO)Mb in solutions, as distinguished from its crystal state. It should be noted that high $\phi(L)$ values are not evidence for the absence of any distortion; they only inform about the absence of E-type distortions in the ground state (cf. refs. 23, 116 and 237).

The vibronic approach also explains the reduction of the quantum yield in the complex $(O_2)^bHb$ by its excitation to the state ψ' with the triply populated $e(d_\pi - \pi_L^*)$ MO [267]. Indeed, this state is lower in energy (by approximately 1 eV) than the Q state, and therefore the intersection of the term E' of this state with the dissociative term E_3 takes place at larger ρ values than that of the Q term. As seen from Fig. 11, in this case the activation barrier increases, lowering the quantum yield.

F. VIBRONIC EFFECTS IN EXCITED *B* AND *Q* STATES

A typical optical absorption spectrum of metalloporphyrins consists of an intense B band (or the Soret band) in the near UV region ($\lambda \approx 400$ nm) and a weak Q band in the visible region ($\lambda \approx 550$ nm). These two bands correspond to electronic transitions from the non-degenerate ground state to the doubly degenerate B and Q states [268,269]. The origin of this spectrum, as well as of some other features, can be explained in the framework of a combination of the four-orbital model suggested by Gouterman [270] with the vibronic approach.

(i) The four-orbital model

As shown in ref. 270, the B and Q states transform as the degenerate representations of the D_{4h} point group and are formed by the exchange interactions of one-electron configurations, which are electron excitations from the highest occupied $a_{2u}(\pi)$ or $a_{1u}(\pi)$ MO to the x and y components of the unoccupied $e_g(\pi^*)$ MO. (Hereafter we denote these configurations as $(a_{2u}e_{gx})$, $(a_{2u}e_{gy})$, $(a_{1u}e_{gx})$ and $(a_{1u}e_{gy})$ respectively.) It is convenient to present the wavefunctions of the B and Q states in the following form (only the y components are given, the x components being similar):

$$B_y = B_y^0 \cos \nu + Q_y^0 \sin \nu$$

$$Q_y = -B_y^0 \sin \nu + Q_y^0 \cos \nu \tag{75}$$

where B_y^0 and Q_y^0 are 50–50 mixtures of the appropriate electronic configurations:

$$B_y^0 = (2)^{-1/2}\left[(a_{2u}e_{gy}) + (a_{1u}e_{gx})\right]$$

$$Q_y^0 = (2)^{-1/2}\left[(a_{2u}e_{gy}) - (a_{1u}e_{gx})\right] \tag{76}$$

and ν is determined by the relationships

$$\sin 2\nu = \Delta_0\left(\beta_0^2 + \Delta_0^2\right)^{-1/2}$$
$$\cos 2\nu = \beta_0\left(\beta_0^2 + \Delta_0^2\right)^{-1/2} \tag{77}$$

Here β_0 is the appropriate exchange integral:

$$\beta_0 = \int (a_{2u}e_{gy})H(a_{1u}e_{gx})\,\mathrm{d}\vec{r} \tag{78}$$

and $2\Delta_0$ is the energy gap between the configurations $(a_{2u}e_{gy})$ and $(a_{1u}e_{gx})$:

$$2\Delta_0 = \mathscr{E}(a_{2u}e_{gy}) - \mathscr{E}(a_{1u}e_{gx}) \tag{79}$$

As shown in ref. 270, the matrix element R_1 of the dipolar transition $a_{1u}(\pi) \rightarrow e_{gx}(\pi^*)$ is approximately equal to that of $a_{2u}(\pi) \rightarrow e_{gy}(\pi^*)$, R_2, and therefore $R_0 \gg r_0$, where

$$R_0 = (2)^{-1/2}(R_1 + R_2);\; r_0 = (2)^{-1/2}(R_2 - R_1) \tag{80}$$

It follows from eqns. (76) and (80) that in compounds with $\sin \nu \ll 1$ (i.e. $\Delta_0/\beta_0 \ll 1$) the intensity of the Q band, determined by the magnitude $(\nu_{R_0 - r_0})^2$, is lower than that of the B band determined by the value R_0^2. This exact situation is observed in metal complexes of a series of porphyrins (porphine, tetraphenylporphine etc.). Moreover, as can easily be shown [270] for small ν values, the energy gap between the B and Q states becomes minimal and equals approximately

$$E_B - E_Q \approx 2\beta_0 \tag{81a}$$

Another situation is observed in complexes of tetrazaporphyrins, in which, owing to the increased Δ_0 value, the inequality $\Delta_0/\beta_0 \ll 1$ is no longer valid. (It should be noted that the β_0 value is weakly dependent on the type of porphyrin [270].) In this case the Q band becomes intense and the energy gap $E_B - E_Q$ increases:

$$E_B - E_Q = 2\left(\beta_0^2 + \Delta_0^2\right)^{1/2} = 2\beta_0/\cos 2\nu \tag{81b}$$

The four-orbital model, in addition to the experimental data mentioned above, also explains the origin of the polarization of light in the B and Q bands and the influence of the peripheral substituents on the shape of the band Q. However, the explicit form of the wavefunctions shows that the magnitudes of the splitting of the B and Q states in low symmetry external fields must be equal to each other [270,271]. However, experimental studies [272–275] show this conclusion to be valid only for complexes of tetrabenzporphins Me(TBP), whereas with other porphyrins the B- and Q-band splitting differs. Below we show that the difference in the splitting of the B and Q states is due to the different vibronic interactions in these two states [276].

(ii) Vibronic effect manifestations

If follows from eqns. (75) and (76) that each of the B and Q states are twofold degenerate and span the E_u representation of the D_{4h} group. Since $[E_u \times E_u] = A_{1g} + B_{1g} + B_{2g}$ and $E_u \times E_u = A_{1g} + B_{1g} + A_{2g} + B_{2g}$, each of these states separately couple with the A_{1g}, B_{1g} and B_{2g} displacements, the interaction with the last two displacements resulting in the Jahn–Teller effect [277,278]. The vibronic intermixing is non-zero for the A_{1g}, B_{1g}, A_{2g} and B_{2g} nuclear displacements (the pseudo-Jahn–Teller effect) [270]. The vibronic intermixing becomes apparent in optical spectroscopy where the vibrational satellite ($0 \rightarrow 1$) of the Q transition occurs due to the admixture of the state B with that of Q [266,269]. It also results in the appearance of resonance Raman scattering peaks due to excitation of non-totally symmetric vibrations in the $Q(0 \rightarrow 0)$ region [279].

The magnitude of the vibronic mixing between the B and Q states was calculated [280] in the cyclic polyene model, and it was shown that these states can only be mixed by non-totally symmetric vibrations. It follows from the four-orbital model (eqn. (76)) that the matrix elements of non-totally symmetric one-electron operators, calculated with each of the B^0 and Q^0 functions, equal zero [270,271,281,282]. Therefore the matrix elements for the mixing of the B and Q states, as seen from eqn. (75), are proportional to $\cos 2\nu$. Hence strong mixing is expected in complexes with small ν values, i.e. with rather different B and Q band intensities. For large ν values the mixing is weak. Both these conclusions are confirmed by experimental data [268,269,283,284].

In the case of Me(TBP) where $\cos 2\nu \approx 0.7$ [271] the phonon satellites are weak in emission only [273], whereas in absorption they are strong. One explanation may be interference between the Franck–Condon transition and the vibronically induced part [273]. It should be noted that in Me(TBP) complexes the Jahn–Teller effect, permitting the Franck–Condon Q ($0 \rightarrow 1$) transition, is much stronger than in porphyrins with small ν values (see below).

According to eqn. (75), the matrix elements of non-totally symmetric one-electron operators within each of the B and Q states are proportional to $\sin 2\nu$. Hence the Jahn–Teller effect is expected to be strong enough in compounds with intermediate values of $\sin 2\nu$, e.g. in Me(TBP), and weak for small ν values [270,285]. However, in spite of its weakness, the Jahn–Teller effect was positively identified in the Q state of Zn(Por) [286,287], Mg(Por) [274], ethanol-Mg(Por) [288] and Cd(TBP) [273] by means of low temperature Zeeman spectroscopy in Shpol'skii matrices. The polarized low temperature fine structure fluorescence spectra of Zn(Por) and Pd(Por) in *n*-octane [289] confirm the presence of distortion along the B_{1g}

displacement. The resonance Raman spectra testify to the Jahn–Teller instability in the Q state of $\mathrm{Ni^{II}(EtioP)}$ and $\mathrm{ClCr^{III}(TPP)}$ [279,290] as well as $\mathrm{(py)_2Me(OEP)}$ (Me = Fe(II), Ru(II), Os(II)) [291].

In the excited triplet state of the porphyrin ring, the Jahn–Teller effect is expected to be stronger [285] owing to the absence of exchange mixing of appropriate one-electron configurations, $\sin 2\nu = 1$. However, experiments in magnetic fields give no direct information about the magnitude of the Jahn–Teller effect, since the main contribution to the splitting of the electronic states in this case is due to the interaction of the magnetic field with the spin subsystem [286, 292]. The proper Jahn–Teller effect here is expressed by the so-called vibronic reduction factors [1,4,6,7], reducing the main electronic quantities: the orbital moment, spin–orbital interaction etc. However, the zero-field splitting reveals the symmetry of the displacements along which the system is distorted.

For instance, Zeeman effect measurements show that in the ^4E_u state of Cu(Por) the distortion is of B_{1g} symmetry [293], whereas in the ^3E_u state of Pd(Por) and Pt(Por) it is of B_{2g} symmetry [293,294]. The electron spin resonance (ESR) spectra in the ^3E_u and ^4E_u states confirm these results [295] and show that in the triplet states of Zn(Por) and Mg(Por) the distortions are of B_{1g} symmetry [292,296]. However, from the low temperature fluorescence spectra of the singlet $Q(^1E_u)$ state of Pd(Por), in *n*-octane, the distortion is of B_{1g} symmetry [289]. It is rather difficult to explain why in Pd(Por) the B_{2g} type distortion in the ^3E_u state changes to the B_{1g} distortion in the ^1E_u state.

The Jahn–Teller effect on the Zeeman splitting in metalloporphyrins introduced into Shpol'skii matrices was considered theoretically in refs. 286–287. It was shown that owing to the vibronic interaction the orbital moment of the system is reduced and the two components of the split Q state behave differently in the magnetic field. A comparison of the theoretical with the experimental results yields the value α_Q:

$$\alpha_Q = 2q_Q/a_Q \tag{82}$$

where q_Q and a_Q are, respectively, the displacement of the minimum position (the distortion) and the amplitude of zeroth vibrations along the Jahn–Teller coordinate. The α_Q values are given in Table 2.

Many papers are devoted to investigation of the resonance Raman spectra of metalloporphyrins [279,281,282,297–305]. Briefly, the results are as follows. Owing to the Jahn–Teller effect, the usual selection rules break down [1,6,7], and the Franck–Condon transitions to excited states with excitation of one or more vibrational quanta of Jahn–Teller active vibrations become possible. This is also true for light scattering in the region of the $Q(0 \rightarrow 0)$ and B transitions [279,281,282,290,306]. In refs. 298, 299 and 306 it is shown

TABLE 2

Numerical values of parameters determining the splitting of the B and Q bands

	α_Q	$\hbar\omega_Q$ (cm^{-1})	$\beta_0/\cos 2\nu$ (cm^{-1})	$\tan 2\nu$	p	η (theoretical)	η (experimental)
Zn(Por)	1.1 [287]	180 [287]	3575 [308]	0.15 [308]	0.40	2.33	2.14 [275]
Mg(Por)	0.7 [274]	193 [274]	3650 [308]	0.06 [308]	0.64	4.55	–
Cd(TBP)	1.27 [273]	150 [273]	4200 [307]	1 [271]	0	1	0.86 [273]

that the multimode vibronic interaction with the totally symmetric vibrations affects the shape of the Raman excitation profiles. Moreover, the simultaneous effect of vibronic interactions and low symmetry external fields may lead to the dispersion of the depolarization of light scattered by vibronic active modes [301,303] (see also ref. 3). The influence of low symmetry external fields is investigated also in ref. 281; in this work some of the requirements of the four-orbital model (the relationship between the matrix elements of the same one-electron operator calculated by different functions of the B and Q states) are violated.

(iii) Simultaneous effect of vibronic interactions and low symmetry external fields

Let us consider the combined influence of an external field of B_{1g} symmetry and vibronic interactions with displacement of the same symmetry on the adiabatic potentials in the excited B and Q states of metalloporphyrins. Using the explicit form of the wavefunctions of the electronic B and Q states (eqn. (75)), we can obtain for the Hamiltonian of interactions with the displacement q and with the external field W, on the basis of these functions, the following matrix expression [282]:

$$H=\left|\begin{array}{cccc} -(\beta_o/\cos 2\nu) & 0 & (fq+V)\cos 2\nu & 0 \\ -(fq+V)\sin 2\nu & & & \\ 0 & -(\beta_0/\cos 2\nu) & 0 & -(fq+V)\cos 2\nu \\ & +(fq+V)\sin 2\nu & & \\ (fq+V)\cos 2\nu & 0 & (\beta_0/\cos 2\nu) & 0 \\ & & +(fq+V)\sin 2\nu & \\ 0 & -(fq+V)\cos 2\nu & 0 & (\beta_0/\cos 2\nu) \\ & & & -(fq+V)\sin 2\nu \end{array}\right| \tag{83}$$

where

$$f = \langle e_{gx} | (\partial H/\partial q)_0 | e_{gx} \rangle$$

$$V = \langle e_{gx} | W | e_{gx} \rangle$$

For the eigenvalues of this Hamiltonian the following expressions can be deduced:

$$\mathscr{E}_{Q_x(Q_y)} = -\left[(\beta_0/\cos 2\nu)^2 + (fq + V)^2 \pm 2\beta_0(fq + V)\tan 2\nu\right]^{1/2}$$

$$\mathscr{E}_{B_x(B_y)} = \left[(\beta_0/\cos 2\nu)^2 + (fq + V)^2 \pm 2\beta_0(fq + V)\tan 2\nu\right]^{1/2} \tag{84}$$

It is seen from eqn. (75) that in the absence of vibronic interactions, the force constants of the B and Q states differ little and depend weakly on the ν value. Therefore we assume that without the vibronic interactions the force constants for the B_{1g} displacement are the same in the B and Q states and equal to K_0 which is independent of ν. Then, using eqn. (84), we can obtain the adiabatic potentials of the components of split B and Q states by adding to $\mathscr{E}$ the elastic energy $\frac{1}{2}K_0q^2$. For the sake of convenience we assume that

$$[(fq + V)\cos 2\nu/\beta_0]^2 < 1 \tag{85}$$

Expanding the expressions for $\mathscr{E}$ according to eqn. (84) in a series with respect to the parameter given by eqn. (85) and keeping terms to second order only, we obtain the following expressions for the adiabatic potentials of the components of the B and Q states:

$$\begin{aligned} E_{Q_x(Q_y)} = {} & -(\beta_0/\cos 2\nu) - (V^2/2\beta_0)\cos^3 2\nu \\ & \mp V\sin 2\nu - \left[(V/\beta_0)\cos^3 2\nu \pm \sin 2\nu\right] fq + (2)^{-1}(1 - p)K_0q^2 \\ E_{B_x(B_y)} = {} & (\beta_0/\cos 2\nu) + (V^2/2\beta_0)\cos^3 2\nu \pm V\sin 2\nu \\ & + \left[(V/\beta_0)\cos^3 2\nu \mp \sin 2\nu\right] fq + (2)^{-1}(1 + p)K_0q^2 \end{aligned} \tag{86}$$

where p is the magnitude of the pseudo-Jahn–Teller softening

$$p = \frac{f^2}{K_0\beta_0}\cos^3 2\nu \tag{87}$$

It follows from eqn. (86) that the force constants of the q displacement are the same for the two components of the Q state, but differ from that of the two components of the B state, the latter also being equal to each other:

$$\begin{aligned} K_Q &= K_0(1 - p) \\ K_B &= K_0(1 + p) \end{aligned} \tag{88}$$

Also from eqn. (86) the expressions for the energy differences between the minima of the adiabatic potentials may be obtained:

$$\Delta E_Q = E_{Q_y}^{\min} - E_{Q_x}^{\min} = 2V \sin 2\nu + 2Vp(1-p)^{-1} \sin 2\nu$$

$$= 2V(1-p)^{-1} \sin 2\nu$$

$$\Delta E_B = E_{B_y}^{\min} - E_{B_x}^{\min} = -2V \sin 2\nu + 2Vp(1-p)^{-1} \sin 2\nu$$

$$= -2V(1+p)^{-1} \sin 2\nu \tag{89}$$

It is seen that two terms contribute to the ΔE_Q and ΔE_B values: the first describes the influence of the external field; it is also non-zero when the vibronic interactions are absent and it changes sign passing from the Q to the B state. The second term describes the combined action of the external field and vibronic effects; it has the same sign in the B and Q states, but is always larger in the latter case than in the former. In the Q state both effects are summed, whereas in the B state the first effect (term) is subtracted from the second. This circumstance leads to the conclusion (emerging directly from eqn. (89)) that for any parameter values the following relations hold: $|\Delta E_Q| \geqslant 2|V \sin 2\nu| \geqslant |\Delta E_B|$, the inequality being valid in the case of the non-zero pseudo-Jahn–Teller effect ($p > 0$).

(iv) Splitting of the B and Q absorption bands

Figure 13 illustrates the light-induced 0 → 0 transitions from the ground state to the B and Q states. The splitting in each of the Q and B bands under the influence of the low symmetry field is determined by the shift in the energy of the x-polarized states with respect to the y-polarized states. The magnitudes of vibrational quanta of Q_x and Q_y (as well as B_x and B_y) are equal, since they have the same force constants (eqn. (88)). As a result the magnitude of the Q (or B) band splitting is determined by the energy difference of the minima of the adiabatic potentials of the Q_x and Q_y (or B_x and B_y) states given by eqn. (89).

It follows from eqn. (89) that the ratio η between the splitting of the Q and B bands in external fields is

$$\eta = \frac{|\Delta E_Q|}{|\Delta E_B|} = \frac{1+p}{1-p} \tag{90}$$

(It follows from eqn. (86) that the ratio of the coordinate differences of the minima of the x and y components of the split Q state to that of the B state is also equal to the η value.) The parameter η for different Me(P) can be obtained from the numerical values of the $\hbar\omega_Q$ frequencies of the Jahn–Teller

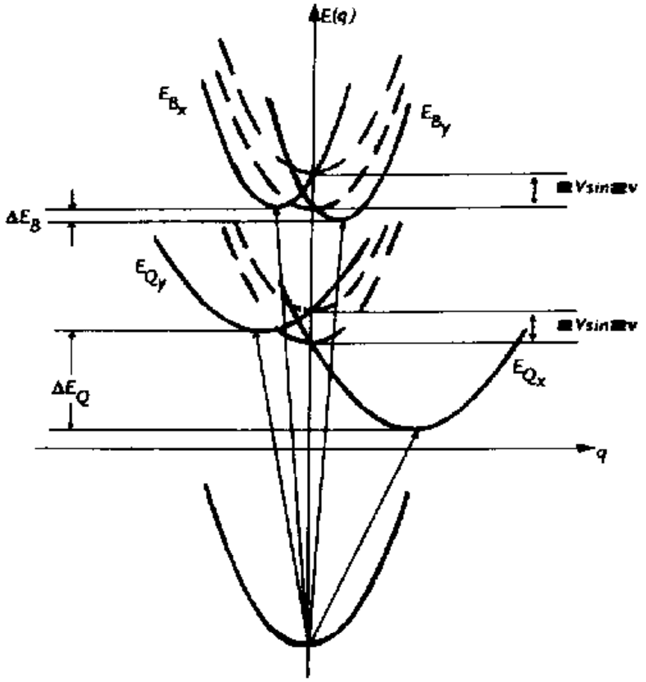

Fig. 13. Optical 0 → 0 transitions to the B and Q states in the presence of low symmetry fields neglecting (broken curves) and taking account of (solid curves) vibronic interactions with displacements of the same symmetry.

B_{1g} vibration in the Q state, the Jahn–Teller distortion α_Q where [273,274,286,287]

$$\alpha_Q = 2\,|\sin 2\nu\,| \left(\frac{f^2}{K_Q} \frac{1}{\hbar \omega_Q} \right)^{1/2} \tag{91}$$

and parameters ν and β_0 [271,307,308]. Indeed, from eqns. (87), (88) and (91) we obtain p:

$$p = \left(1 + \frac{4 \tan^2 2\nu}{\alpha_Q^2 \hbar \omega_Q} \frac{\beta_0}{\cos 2\nu} \right)^{-1} \tag{92}$$

Some numerical estimates of η are given in Table 2. It is seen that in complexes of tetrabenzporphin the splitting of the Q and B terms by the external field are expected to differ weakly ($\eta = 1$), whereas in Zn(Por) and Mg(Por) this difference must be large ($\eta = 2.33$ and $\eta = 4.55$ respectively). This conclusion is confirmed by experimental data on B- and Q-band splitting in n-alkanes [273,275] (see also Table 2). The dispersion of experimental values of η for Zn(Por) may be due to the influence of the B_{2g} component of the crystal field in A sites of n-alkanes [287] (not taken into account in the calculations), which is different in different crystals. It is expected to be reduced more by interactions with the B_{1g} displacement in the Q than in the B state. Indeed, the vibronic reduction factors in the Q and B states are $\exp(-\alpha_Q^2/4)$ and $\exp(-\alpha_B^2/4)$ respectively [286], where α_Q is given in eqn. (91) and α_B, similarly, is

$$\alpha_B = 2\,|\sin 2\nu|\left(\frac{f^2}{K_B}\frac{1}{\hbar\omega_B}\right)^{1/2} \tag{93}$$

It follows from eqns. (88), (90), (91) and (93) that

$$\frac{\alpha_Q}{\alpha_B} = \left(\frac{K_B}{K_Q}\frac{\omega_B}{\omega_Q}\right)^{1/2} = \left(\frac{K_B}{K_Q}\right)^{3/4} = \eta^{3/4} \tag{94}$$

Since $\eta = 2.33$ (Table 2), the vibronic reduction in the Q state is about 1.5 times stronger than in the B state. The fact that the ratio of the Q- and B-band splitting in the B sites of n-alkanes is less than unity [275] does not contradict our results and can be explained in the above scheme with the assumption that in the B sites the crystal field of the Shpol'skii matrix has a predominant B_{2g} component. The observed η value in Cd(TBP), which is slightly less than unity, is presumably due to the contribution of orbitals not included in the four-orbital model [309].

The change in the p parameter on passing from Zn(Por) to Mg(Por) can be explained, perhaps, by a small (about 20%) increase in the orbital vibronic constant (see Section B) in Mg(por). Using eqn. (89) and assuming that the orbital matrix element of the crystal field of n-octane does not change passing from Zn(Por) to Mg(Por), the ratio between the Q band splitting of metalloporphins in the external field can be estimated:

$$\frac{\Delta E_Q(\mathrm{Zn})}{\Delta E_Q(\mathrm{Mg})} = \frac{\sin 2\nu(\mathrm{Zn})}{\sin 2\nu(\mathrm{Mg})}\,\frac{1-p(\mathrm{Mg})}{1-p(\mathrm{Zn})} = 1.5$$

The experiment yields a value $\Delta E_Q(\mathrm{Zn})/\Delta E_Q(\mathrm{Mg}) = 1.8$ [274,287], confirming that the orbital matrix element of the crystal field changes little by substituting the Zn by the Mg atom.

Thus the vibronic approach explains the difference in Q- and B-band splitting in low symmetry fields as due to the difference in the Jahn–Teller distortions of the system in these two states. The results of ref. 310 also support the contribution of such a distortion to the splitting of the Q band.

The vibronic approach also explains the rather greater splitting of the Q band (about 2960 cm^{-1} [270]) than that of the B band (from 240 cm^{-1} [270] to 500 cm^{-1} [311]) when substitution of the metal by two protons takes place. Indeed, the two protons in H_2(TPP) produce an additional field of B_{1g} symmetry [270]. Following from these arguments, the combined action of the vibronic interactions and the low symmetry fields leads to different splitting of the B and Q bands. The different splitting of the B and Q bands in free base porphins [270,311] and almost equal splitting in H_2(TBP) [269,307] can be explained to be due to the differences in the magnitude of the pseudo-Jahn–Teller effect and hence in the η values (see Table 2). From this point of view the two-electron integrals only increase the difference between ΔE_Q and ΔE_B in these compounds. The direct quantum-chemical calculation of the optical absorption spectra of free-base porphyrins, without taking account of the different nuclear configurations in the B and Q states [312–318] show that ΔE_Q and ΔE_B may differ by no more than a factor of 2.5. Moreover, following from eqn. (89) in the systems under consideration there is the vibronic amplification effect of electronic operators distinguished from the usual vibronic reduction effect thereof.

G. CONCLUDING REMARKS

In this review we have tried to present a systematic approach to the explanation of many properties and regularities of metalloporphyrins and hemoproteins. This approach, based on the vibronic interaction theory, establishes a direct correlation between the electronic structure of the complexes under consideration and the stability (or instability) of their nuclear configuration. In this correlation the most important criterion is the pseudo-Jahn–Teller (vibronic) instability of the high symmetry configurations. In the framework of this approach, understanding is achieved for the origin of the observed stereochemistry, ground state spin multiplicity, the influence of axial ligands, the principal features of photodecay, absorption band splitting in different derivatives of metalloporphyrins and active centres of hemoproteins etc.

The following are currently unsolved problems.

For some of the systems considered in this paper the estimates and comparisons of observable magnitudes were carried out in a qualitative way. Although the qualitative conclusions based on a comparison of these relative magnitudes obtained within a series of similar compounds are convincing, more rigorous numerical estimates of some of the quantities under consideration seem to be necessary. These include, for example, estimation of the coordination geometry of diatomics, more accurate determination of the adiabatic potential surface of the excited state responsible for the photodecay of diatomics, calculation of the displacement of the metal atom from the porphyrin ring etc.

The vibronic approach opens the way for solutions of some problems that have not yet been considered. Among them the problem of chemical activation of small molecules by coordination to metalloenzymes is very important. This problem can be considered by means of the vibronic theory in a similar fashion to the case of coordination to the usual transition metal complexes (see Section B). The conclusions of Section F can be used directly for the investigation of the magnetic circular dichroism spectra, resonance Raman scattering, Zeeman effect etc., in the *B* and *Q* bands, that have as yet had no proper treatment.

Special attention should be paid to the results which stimulate new experimental work. These include prediction of the in-plane position of the metal atoms with occupied d_{z^2} orbitals (atoms with d^9, d^{10} and low spin d^8 electronic configurations) partially confirmed by experimental data. Not yet confirmed are predictions of the highly excited rotational states of the photodissociated diatomics (CO, NO) immediately after dissociation, of the relationship between the splitting magnitudes of the zero-phonon transitions to the *B* and *Q* states and of the weak influence of the iron charge ($Fe^{2+} \rightleftarrows Fe^{3+}$) on its position with respect to the heme plane etc.

REFERENCES

1 I.B. Bersuker, The Jahn–Teller Effect and Vibronic Interactions in Modern Chemistry, Plenum, New York, 1984.
2 H. Köppel, W. Domcke and L.S. Cederbaum, Adv. Chem. Phys., 57 (1984) 59.
3 I.B. Bersuker and I.Ya. Ogurtsov, Adv. Quantum Chem., 18 (1986) 1.
4 I.B. Bersuker (Ed.), The Jahn–Teller Effect. A Bibliographic Review, IFI Plenum, New York, 1984.
5 I.B. Bersuker, Electronic Structure and Properties of Coordination Compounds, Khimia, Leningrad, 1986 (in Russian).
6 R. Englman, The Jahn–Teller Effect in Molecules and Crystals, Wiley, New York, 1972.
7 I.B. Bersuker and V.Z. Polinger, Vibronic Interactions in Polyatomic Systems, Nauka, Moscow, 1983 (in Russian).
8 I.B. Bersuker, Russ. Chem. Rev., 55 (1986) 581.
9 I.B. Bersuker, Nouv. J. Chim., 4 (1980) 139.
10 I.B. Bersuker, N.N. Gorinchoy and V.Z. Polinger, Theor. Chim. Acta, 66 (1984) 161.
11 T.K. Rebane, Teor. Eksp. Khim., 20 (1984) 532.
12 R. Pearson, Symmetry Rules for Chemical Reactions, Wiley, New York, 1976.
13 J.L. Hoard, in K.M. Smith (Ed.), Porphyrins and Metalloporphyrins, Elsevier, Amsterdam, 1975, p. 317.
14 W.R. Scheidt, in D. Dolphin (Ed.), The Porphyrins, Vol. 3, Academic Press, New York, 1978, p. 463.
15 T.G. Traylor, Acc. Chem. Res., 14 (1981) 102.
16 J.L. Hoard, in D.A. Adler (Ed.), Ann. N. Y. Acad. Sci., 206 (1973) 18.
17 W.R. Scheidt and C. Reed, Chem. Rev., 81 (1981) 543.
18 J.L. Hoard, M.J. Hamor and T.A. Hamor, J. Am. Chem. Soc., 85 (1967) 2334.
19 M.F. Perutz, H. Muirhead, J.N. Cox and L.C.G. Goaman, Nature, 219 (1968) 131.
20 M.F. Perutz, Nature, 228 (1970) 726.
21 M.F. Perutz, Nature, 237 (1972) 495.
22 M.F. Perutz, Br. Med. Bull., 32 (1976) 195.

23 M.F. Perutz, Annu. Rev. Biochem., 48 (1979) 327.
24 W.R. Scheidt, M.E. Kastner and K. Hatano, Inorg. Chem., 17 (1978) 706.
25 W.R. Scheidt, J.U. Mondal, C.W. Eigenbrot, A. Adler, L.J. Radonovich and J.L. Hoard, Inorg. Chem., 25 (1986) 795.
26 M.J. Sienko, R.A. Plane and R.E. Hester, Inorganic Chemistry: Principles and Elements, Benjamin, New York–Amsterdam, 1965.
27 (a) J.F. Kirner, W. Daw and W.R. Scheidt, Inorg. Chem., 15 (1976) 1685.
(b) W.R. Scheidt and W. Dow, J. Am. Chem. Soc., 99 (1977) 1101.
28 J.F. Kirner, C.A. Reed and W.R. Scheidt, J. Am. Chem. Soc., 99 (1977) 1093.
29 (a) I.B. Bersuker and S.S. Stavrov, Chem. Phys., 54 (1981) 331.
(b) I.B. Bersuker and S.S. Stavrov, in Proc. 3rd All-Union Conf. on Chemistry and Biochemistry of Porphyrins, Samarkand University, Samarkand, 1983, p. 87 (in Russian).
(c) I.B. Bersuker and S.S. Stavrov, Inorg. Chim. Acta, 79 (1983) 177.
30 M. Zerner, M. Gouterman and H. Kobayashi, Theor. Chim. Acta, 6 (1966) 363.
31 M. Zerner and M. Gouterman, Theor. Chim. Acta, 4 (1966) 44.
32 A.M. Schaffer, M. Gouterman and E.R. Davidson, Theor. Chim. Acta, 30 (1973) 9.
33 M. Gouterman, L.K. Hanson, G.E. Khalil, W.R. Leenstra and J.W. Buchler, J. Chem. Phys., 62 (1975) 2343.
34 E.F. Meyer, Jr., Acta Crystallogr. Sect. B, 28 (1972) 2162.
35 D.L. Cullen and E.F. Meyer, Jr., J. Am. Chem. Soc., 96 (1974) 2095.
36 T.A. Hamor, W.S. Caughey and J.L. Hoard, J. Am. Chem. Soc., 87 (1965) 2305.
37 M. Saito and H. Kashiwagi, J. Chem. Phys., 82 (1985) 848.
38 E.B. Fleischer, C.K. Miller and L.E. Webb, J. Am. Chem. Soc., 86 (1964) 2342.
39 I. Moustakali and A. Tulinsky, J. Am. Chem. Soc., 95 (1973) 6811.
40 I.B. Bersuker, S.S. Stavrov and B.G. Vekhter, in Physical and Mathematical Methods in Coordination Chemistry, Abstracts of the 6th All-Union Conference, Shtiintsa, Kishinev, 1977, p. 139 (in Russian).
41 I.B. Bersuker, S.S. Stavrov and B.G. Vekhter, in Int. Conf. on Quantum Chemistry, Biology and Pharmacology, Abstr. Vol. 4, Acad. Sci. Ukr. SSR, Inst. Theor. Phys., Kiev, 1978, p. 44.
42 I.B. Bersuker, S.S. Stavrov and B.G. Vekhter, Biofizika, 24 (1979) 413.
43 A. Warshel and A. Lappicirella, J. Am. Chem. Soc., 103 (1981) 4664.
44 J.B. Ferraro, Low Frequency Vibrations of Inorganic and Coordination Compounds, Plenum, New York, 1971.
45 K. Nakamoto, Infrared and Raman Spectra of Inorganic and Coordination Compounds, Wiley, New York, 1978.
46 L.J. Boucher and J.J. Katz, J. Am. Chem. Soc., 89 (1967) 1340.
47 W.A. Eaton, L.K. Hanson, P.J. Stephens and J.B.R. Dunn, J. Am. Chem. Soc., 100 (1978) 4991.
48 M. Abe, T. Kitagawa and Y. Kyogoku, J. Chem. Phys., 69 (1978) 4526.
49 P. Madura and W.R. Scheidt, Inorg. Chem., 15 (1976) 3182.
50 P. Doppelt, J. Fischer and R. Weiss, Inorg. Chem., 23 (1984) 2958.
51 S. Ciurli, S. Gambarotta, C. Floriani, A. Chiesi-Villa and G. Guastini, Angew. Chem. Int. Ed. Engl., 25 (1986) 553.
52 I.P. Beletskii and K.B. Yatsimirskii, Teor. Eksp. Khim., 21 (1985) 1.
53 A. Veillard, A. Dedieu and M.-M. Rohmer, in K. Fukui and B. Pullman (Eds.), Horizons of Quantum Chemistry, Reidel, Dordrecht, 1980, p. 197.
54 H. Kashiwagi and S. Obara, Int. J. Quantum Chem., 20 (1981) 843.
55 S. Obara and H. Kashiwagi, J. Chem. Phys., 77 (1982) 3156.

56 M.-M. Rohmer, Chem. Phys. Lett., 116 (1985) 44.
57 W.D. Edwards, B. Weiner and M.C. Zerner, J. Am. Chem. Soc., 108 (1986) 2196.
58 S.F. Sontum, D.A. Case and M. Karplus, J. Chem. Phys., 79 (1983) 2881.
59 H. Goff, G.N. La Mar and C.A. Reed, J. Am. Chem. Soc., 99 (1977) 3641.
60 J. Mispelter, M. Momenteau and J.M. Lhoste, J. Chem. Phys., 72 (1980) 1003.
61 G. Lang, K. Spartalian, C.A. Reed and J.P. Collman, J. Chem. Phys., 69 (1978) 5424.
62 K. Tanaka, E. Elkaim, L. Li, Z.N. Jue, P. Coppens and J. Landrum, J. Chem. Phys., 84 (1986) 6969.
63 T. Kitagawa and J. Teraoka, Chem. Phys. Lett., 63 (1979) 443.
64 J.P. Collman, J.L. Hoard, N. Kim, G. Lang and C.A. Reed, J. Am. Chem. Soc., 97 (1975) 2676.
65 S.H. Stauss, M.E. Silver, K.M. Long, R.C. Thompson, R.A. Hudgens, K. Spartalian and J.A. Ibers, J. Am. Chem. Soc., 107 (1985) 4207.
66 T. Mashiko, C.A. Reed, K.J. Haller and W.R. Scheidt, Inorg. Chem., 23 (1984) 3192.
67 B.D. Olafson and W.A. Goddard III, Proc. Natl. Acad. Sci. U.S.A., 74 (1977) 1315.
68 S. Mizuhashi, J. Theor. Biol., 66 (1977) 13.
69 S. Mizuhashi, J. Phys. Soc. Jpn., 45 (1978) 612.
70 S. Mizuhashi, J. Phys. Soc. Jpn., 52 (1983) 74.
71 S. Mizuhashi, J. Phys. Soc. Jpn., 53 (1984) 3256.
72 M.J.S. Dewar, The Molecular Orbital Theory of Organic Chemistry, McGraw-Hill, New York, 1969.
73 H. Fujimoto and F. Fukui, in G. Klopman (Ed.), Chemical Reactivity and Reaction Paths, Wiley, New York, 1974, p. 30.
74 G. Klopman, in G. Klopman (Ed.), Chemical Reactivity and Reaction Paths, Wiley, New York, 1974, p. 61.
75 J.N. Murrell, S.F. Kettle and J.M. Tedder, The Chemical Bond, Wiley, Chichester, 1978.
76 S.S. Stavrov, Vibronic Effects in Metalloporphyrins and Hemoproteins: Stereochemistry, Coordination and Photolysis, Ph.D. Thesis, Moscow, 1982 (in Russian).
77 S.S. Stavrov and I.B. Bersuker, Inorg. Chim. Acta, 79 (1986) 176.
78 A.A. Levin, A.P. Klyagina and S.P. Dolin, Koord. Khim., 4 (1978) 354.
79 A.A. Levin, A.P. Klyagina and S.P. Dolin, Zh. Neorg. Khim., 24 (1979) 2307.
80 P.N. D'yachkov, Dokl. Akad. Nauk SSSR, 254 (1980) 920.
81 S. Sugano, Y. Tanabe and H. Kamimura, Multiplets of Transition-Metal Ions in Crystals, Academic Press, New York, 1970.
82 A. Tulinsky and B.M. Chen, J. Am. Chem. Soc., 99 (1977) 3647.
83 W.R. Scheidt and M. Gouterman, in A.B.P. Lever and H.B. Gray (Eds.), Iron Porphyrins (Part 1), Addison–Wesley, London, 1983, p. 89.
84 L.K. Hanson, Int. J. Quantum Chem. Quantum Biol. Symp., 6 (1979) 73.
85 L. Eisenstein, D.R. Fraceschetti and K.L. Yip, Theor. Chim. Acta, 49 (1978) 349.
86 C. Caron, A. Mitschler, G. Rivière, L. Ricard, M. Schappacher and R. Weiss, J. Am. Chem. Soc., 101 (1979) 7401.
87 B. Gonzalez, J. Kouba, S. Yee, C.A. Reed, J.F. Kirner and W.R. Scheidt, J. Am. Chem. Soc., 97 (1975) 3247.
88 J.F. Kirner, C.A. Reed and W.R. Scheidt, J. Am. Chem. Soc., 99 (1977) 2557.
89 P. Doppelt, Inorg. Chem., 23 (1984) 4009.
90 G.B. Jameson, F.S. Molinaro, J.A. Ibers, J.P. Collman, J.I. Brauman, E. Rose and K.S. Suslick, J. Am. Chem. Soc., 102 (1980) 3224.
91 D.R. English, D.N. Hendrickson, K.S. Suslick, C.W. Eigenbrot, Jr., and W.R. Scheidt, J. Am. Chem. Soc., 106 (1984) 7258.

92 M. Schappacher, L. Ricard and R. Weiss, God. Jugosl. Cent. Kristalogr., 16 (1981) 21.
93 M. Schappacher, L. Ricard, R. Weiss, R. Montiel-Montoya, U. Gonser, E. Bill and A. Trautwein, Inorg. Chim. Acta, 78 (1983) L9.
94 P.D. Smith, B.R. James and D. Dolphin, Coord. Chem. Rev., 39 (1981) 31.
95 T. Takano, J. Mol. Biol., 110 (1977) 569.
96 G. Fermi, M.F. Perutz, B. Shaanan and F. Fourme, J. Mol. Biol., 175 (1984) 159.
97 J.M. Baldwin and C. Chothia, J. Mol. Biol., 129 (1979) 175.
98 B.R. Gelin and M. Karplus, Proc. Natl. Acad. Sci. U.S.A., 74 (1977) 801.
99 B.R. Gelin, A.W.-M. Lee and M. Karplus, J. Mol. Biol., 171 (1983) 489.
100 W. Steigemann and E. Weber, J. Mol. Biol., 127 (1979) 309.
101 J.C.W. Chien, J. Phys. Chem., 82 (1978) 2171.
102 G. Fermi, M.F. Perutz, L.C. Dickinson and J.C.W. Chien, J. Mol. Biol., 155 (1982) 495.
103 M. Bolognesi, A. Coda, G. Gatti, P. Ascenzi and M. Brunori, J. Mol. Biol., 183 (1985) 113.
104 K.C. Cho and J.J. Hopfield, Biochemistry, 18 (1979) 5826.
105 E.G. Arutyunyan, I. Daizenhofer, A.V. Teplyakov, I.P. Kuranova, G.V. Oblomova and B.K. Vainshtein, Dokl. Akad. Nauk SSSR, 270 (1983) 732.
106 P.C. Weber, A. Howard, N.H. Xuong and F.R. Salemme, J. Mol. Biol., 153 (1981) 399.
107 P.C. Weber, Biochemistry, 21 (1982) 5116.
108 B.C. Finzel, P.C. Weber, K.D. Hardman and F.R. Salemme, J. Mol. Biol., 186 (1985) 627.
109 V. Srajer, K.T. Schomaker and P.M. Champion, Phys. Rev. Lett., 57 (1986) 1267.
110 J.F. Deatherage, R.S. Loe, C.M. Anderson and K. Moffat, J. Mol. Biol., 104 (1976) 687.
111 E.J. Heidner, R.C. Ladner and M.F. Perutz, J. Mol. Biol., 104 (1976) 707.
112 T. Takano, J. Mol. Biol., 110 (1977) 537.
113 R.C. Ladner, E.J. Heidner and M.F. Perutz, J. Mol. Biol., 114 (1977) 385.
114 J.F. Deatherage and K. Moffat, J. Mol. Biol., 134 (1979) 401.
115 J.F. Deatherage, S.K. Obendorf and K. Moffat, J. Mol. Biol., 134 (1979) 419.
116 J.M. Baldwin, J. Mol. Biol., 136 (1980) 103.
117 S.E.V. Phillips, J. Mol. Biol., 142 (1980) 531.
118 Z.R. Korszun and K. Moffat, J. Mol. Biol., 145 (1981) 815.
119 J.A. Bell, Z.R. Korszun and K. Moffat, J. Mol. Biol., 147 (1981) 325.
120 B. Shaanan, J. Mol. Biol., 171 (1983) 31.
121 B.C. Finzel, T.L. Poulos and J. Kraut, J. Biol. Chem., 259 (1984) 13027.
122 R. Swanson, B.L. Trus, N. Mandel, G. Mandel, O.B. Kallai and R.E. Dickerson, J. Biol. Chem., 252 (1977) 759.
123 T. Takano, B.L. Trus, N. Mandel, G. Mandel, O.B. Kallai, R. Swanson and R.E. Dickerson, J. Biol. Chem., 252 (1977) 776.
124 N. Mandel, G. Mandel, B.L. Trus, J. Rosenberg, G. Carlson and R.E. Dickerson, J. Biol. Chem., 252 (1977) 4619.
125 T. Takano and R.E. Dickerson, Proc. Natl. Acad. Sci. U.S.A., 77 (1980) 6371.
126 Y. Matsuura, T. Takano and R.E. Dickerson, J. Mol. Biol., 156 (1982) 389.
127 Y. Higuchi, M. Kusunoki, Y. Matsuura, N. Yasuoka and M. Kakudo, J. Mol. Biol., 172 (1984) 109.
128 C.-M. Wang and W.S. Brinigar, Biochemistry, 18 (1979) 4960.
129 A. Warshel, Proc. Natl. Acad. Sci. U.S.A., 74 (1977) 1789.
130 G.H. Loew and R.F. Kirchner, Biophys. J., 22 (1978) 179.
131 S. Mizuhashi, Rep. Univ. Electro-Comm., 36 (1986) 253.
132 M. Weissbluth, Hemoglobin. Cooperativity and Electronic Properties, Chapman and Hall, London, 1974.

133 L. Cianchi, M. Mancini and G. Spina, Lett. Nuovo Cimento, 15 (1976) 263.
134 L. Cianchi, F. Gulisano, M. Mancini and G. Spina, Phys. Lett. A, 59 (1976) 247.
135 J.P. Collman, Acc. Chem. Res., 10 (1977) 265.
136 T.D. Smith and J.R. Pilbrow, Coord. Chem. Rev., 39 (1981) 295.
137 L.K. Hanson and B.M. Hoffman, J. Am. Chem. Soc., 102 (1980) 4602.
138 B.M. Hoffman, C.J. Weschler and F. Basolo, J. Am. Chem. Soc., 98 (1976) 5473.
139 T. Watanabe, T. Ama and K. Nakamoto, Inorg. Chem., 22 (1983) 2470.
140 I.B. Bersuker and S.S. Stavrov, in Physical and Mathematical Methods in Coordination Chemistry. Abstr. of the 7th All-Union Conf., Shtiintsa Kishinev, 1980, p. 280 (in Russian).
141 B.B. Wayland, J.V. Minkiewicz and M.E. Abd-Elmageed, J. Am. Chem. Soc., 96 (1974) 2795.
142 B.B. Wayland and D. Mohajer, J. Am. Chem. Soc., 93 (1971) 5295.
143 S.M. Peng and J.A. Ibers, J. Am. Chem. Soc., 98 (1976) 8032.
144 W.R. Scheidt, K.J. Haller, M. Fons, T. Mashiko and C.A. Reed, Biochemistry, 20 (1981) 3563.
145 A. Schweiger, E. Jörin and H.S. Gunthard, in S. Kundla, E. Lippmaa and T. Saluvere (Eds.), Magnetic Resonance and Related Phenomena, Proc. XX Congress AMPERE, Tallin, 1978, Springer, Berlin, 1979, p. 525.
146 J.P. Collman, R.R. Gagne, C.A. Reed, W.T. Robinson and G.A. Rodley, Proc. Natl. Acad. Sci. U.S.A., 71 (1974) 1326.
147 J.P. Collman, R.R. Gagne, C.A. Reed, T.R. Halbert, G. Lang and W.T. Robinson, J. Am. Chem. Soc., 97 (1975) 1427.
148 L. Ricard, M. Schappacher, R. Weiss, R. Montiel-Montoya, E. Bill, U. Gonser and A. Trautwein, Nouv. J. Chim., 7 (1983) 405.
149 G.B. Jameson, G.A. Rodley, W.T. Robinson, R.R. Gagne, C.A. Reed and J.P. Collman, Inorg. Chem., 17 (1978) 850.
150 H. Frauenfelder and G.A. Petsko, Biophys. J., 32 (1980) 465.
151 S.K. Cheung, C.J. Grimes, J. Wong and C.A. Reed, J. Am. Chem. Soc., 98 (1976) 5028.
152 W.R. Scheidt and J.L. Hoard, J. Am. Chem. Soc., 95 (1973) 8281.
153 W.R. Scheidt and M.E. Frisse, J. Am. Chem. Soc., 97 (1975) 17.
154 W.R. Scheidt and P.L. Piciulo, J. Am. Chem. Soc., 98 (1976) 1913.
155 W.R. Scheidt, A.C. Brinegar, E.B. Ferro and J.F. Kirner, J. Am. Chem. Soc., 99 (1977) 7315.
156 W.R. Scheidt, K. Hatano, G.A. Rupprecht and P.L. Piciulo, Inorg. Chem., 18 (1979) 292.
157 W.R. Scheidt, Y.J. Lee and K. Hatano, J. Am. Chem. Soc., 106 (1984) 3191.
158 U. Öpik and M.N.L. Pryce, Proc. Roy. Soc. London, Ser. A, 238 (1957) 425.
159 K. Spartalian, G. Lang, J.P. Collman, R.R. Gagne and C.A. Reed, J. Chem. Phys., 63 (1975) 5375.
160 G. Lang and K. Spartalian, in Mössbauer Effect Methodology, Vol. 10, Proc. 10th Symp., New York, 1976, p. 169.
161 T.G. Traylor and A.P. Berzinies, Proc. Natl. Acad. Sci. U.S.A., 77 (1980) 3171.
162 J.P. Collman, J.I. Brauman, T.R. Halbert and K.S. Suslick, Proc. Natl. Acad. Sci. U.S.A., 73 (1976) 3333.
163 H. Hori, M. Ikeda-Saito and T. Yonetani, Nature, 288 (1980) 501.
164 H. Hori, M. Ikeda-Saito and T. Yonetani, J. Biol. Chem., 256 (1981) 7849.
165 H. Hori, M. Ikeda-Saito and T. Yonetani, J. Biol. Chem., 257 (1982) 3636.
166 F.A. Walker and J. Bowen, J. Am. Chem. Soc., 107 (1985) 7632.
167 J.H. Enemark and R.D. Feltham, Coord. Chem. Rev., 13 (1974) 339.

168 B.B. Wayland and L.W. Olson, J. Am. Chem. Soc., 96 (1974) 6037.
169 D.M.P. Mingos, Inorg. Chem., 12 (1973) 1209.
170 R. Hoffman, M.M.L. Chen, M. Elian, A.R. Rossi and D.M.P. Mingos, Inorg. Chem., 13 (1974) 2666.
171 A. Dedieu and M.-M. Rohmer, J. Am. Chem. Soc., 99 (1977) 8050.
172 G.H. Loew and R.F. Kirchner, Int. J. Quantum Chem. Quantum Biol. Symp., 5 (1978) 403.
173 A. Dedieu, M.-M. Rohmer, H. Veillard and A. Veillard, Nouv. J. Chim., 3 (1979) 653.
174 N.H. Sabelli and C.A. Meledres, J. Phys. Chem., 86 (1982) 4342.
175 J.E. Newton and M.B. Hall, Inorg. Chem., 23 (1984) 4627.
176 J.E. Newton and M.B. Hall, Inorg. Chem., 24 (1985) 2573.
177 A.P. Mineyev, Yu.A. Sharonov, N.A. Sharonova and V.A. Figlovsky, Int. J. Quantum Chem., 16 (1979) 883.
178 S. Mizuhashi, J. Phys. Soc. Jpn., 26 (1969) 468.
179 B.D. Bhattacharyya, Phys. Status Solidi B, 74 (1976) 695.
180 M. Bacci, Chem. Phys. Lett., 48 (1977) 184.
181 M. Bacci, J. Chem. Phys., 68 (1978) 4907.
182 M. Bacci, Biophys. Chem., 11 (1980) 39.
183 D. Cintolesi and M. Mancini, Lett. Nuovo Cimento, 34 (1982) 145.
184 T. Kent, K. Spartalian, G. Lang and T. Yonetani, Biochim. Biophys. Acta, 490 (1977) 331.
185 T.A. Kent, K. Spartalian, G. Lang, T. Yonetani, C.A. Reed and J.P. Collman, Biochim. Biophys. Acta, 580 (1979) 245.
186 T.A. Kent, K. Spartalian and G. Lang, J. Chem. Phys., 71 (1979) 4899.
186 (a) G.I. Bersuker and V.Z. Polinger, Chem. Phys., 86 (1984) 57.
187 B.G. Malmström, Biochim. Biophys. Acta, 549 (1979) 281.
188 L.J. Parkhurst, Annu. Rev. Phys. Chem., 30 (1979) 503.
189 R.M. Davydov, in Redox Metalloenzymes and Their Models. Theoretical and Methodological Aspects, Part 2, Nauka, Chernogolovka, 1982, p. 55 (in Russian).
190 L.A. Blumenfeld, in Molecular Interactions and Activity in Proteins, Excerpta Medica, Amsterdam, 1978, p. 47.
191 R. Boelens and R. Wever, Biochim. Biophys. Acta, 547 (1979) 296.
192 S. Kawato, E. Sigel, E. Carafoli and R.J. Cherry, J. Biol. Chem., 255 (1980) 5508.
193 J.M. Friedman, D.L. Rousseau and M.R. Ondrias, Annu. Rev. Phys. Chem., 33 (1982) 471.
194 C.K. Chang and D. Dolphin, Proc. Natl. Acad. Sci. U.S.A., 73 (1976) 3338.
195 D. Keilin and E.F. Hartree, Biochem. J., 61 (1955) 153.
196 Q.H. Gibson and S. Ainsworth, Nature, 180 (1957) 1416.
197 Q.H. Gibson, in D. Dolphin (Ed.), The Porphyrins, Vol. 5, Academic Press, New York, 1978, p. 153.
198 R.H. Austin, K.W. Beeson, L. Eisenstein, H. Frauenfelder and I.C. Gunsalus, Biochemistry, 14 (1975) 5355.
199 N. Alberding, R.H. Austin, S.S. Chan, L. Eisenstein, H. Frauenfelder, I.C. Gunsalus and T.M. Nordlund, J. Chem. Phys., 65 (1976) 4701.
200 N. Alberding, S.S. Chan, L. Eisenstein, H. Frauenfelder, D. Good, I.C. Gunsalus, T.M. Nordlund, M.F. Perutz, Q.H. Reynolds and L.B. Sorensen, Biochemistry, 17 (1978) 13.
201 J.O. Alben, D. Beece, S.F. Bowne, L. Eisenstein, H. Frauenfelder, D. Good, M.C. Marden, P.P. Moh, L. Reinisch, A.H. Reynolds and K.T. Yue, Phys. Rev. Lett., **44** (1980) 1157.

202 B. Alpert, S. El Mohsni, E. Lindqvist and F. Tfibel, Chem. Phys. Lett., 64 (1979) 11.
203 T. Iizuka, H. Yamamoto, M. Kotani and T. Yonetani, Biochim. Biophys. Acta, 351 (1974) 182.
204 B.M. Hoffman and Q.H. Gibson, Proc. Natl. Acad. Sci. U.S.A., 75 (1978) 21.
205 Q.H. Gibson and B.M. Hoffman, J. Biol. Chem., 254 (1979) 4691.
206 S. Greschner, R.M. Davydov, G.-R. Jänig, K. Ruckpaul and L.A. Blumenfeld, Zh. Fiz. Khim., 56 (1982) 2884.
207 L.A. Blumenfeld, Yu.A. Ermakov and V.J. Passechnik, Biofizika, 22 (1977) 8.
208 K.B. Lyons, J.M. Friedman and P.A. Fleury, Nature, 275 (1978) 565.
209 J.M. Friedman and K.B. Lyons, Nature, 284 (1980) 570.
210 J. Terner, T.G. Spiro, M. Nagumo, M.F. Nicol and M.A. El-Sayed, J. Am. Chem. Soc., 102 (1980) 3238.
211 J. Terner, J.D. Stong, T.G. Spiro, M. Nagumo, M. Nicol and M.A. El-Sayed, Proc. Natl. Acad. Sci. U.S.A., 78 (1981) 1313.
212 J. Terner, D.F. Voss, C. Paddock, R.B. Miles and T.G. Spiro, J. Phys. Chem., 86 (1982) 879.
213 J.M. Friedman, T.W. Scott, G.J. Fisanick, S.R. Simon, E.W. Findsen, M.R. Ondrias and V.W. McDonald, Science, 229 (1985) 187.
214 E.W. Findsen, J.M. Friedman, M.R. Ondrias and S.R. Simon, Science, 229 (1985) 661.
215 Yu.A. Sharonov, Mol. Biol. (Moscow), 20 (1986) 440.
216 Yu.A. Sharonov, V.Z. Pismensky, S. Greschner and K. Ruckpaul, Mol. Biol. (Moscow), 20 (1986) 451.
217 F. Siebert, W. Mantele and W. Kreutz, Biophys. Struct. Mech., 6 (1980) 139.
218 H.-E. Marcolin, R. Reschke and A. Trautwein, Eur. J. Biochem., 96 (1979) 119.
219 B. Chance, R. Fischetti and L. Powers, Biochemistry, 22 (1983) 3820.
220 L. Powers, J.L. Sessler, G.L. Woolery and B. Chance, Biochemistry, 23 (1984) 5519.
221 H. Roder, J. Berendzen, S.F. Bowne, H. Frauenfelder, T.B. Sauke, E. Shyamsunder and M.B. Weissman, Proc. Natl. Acad. Sci. U.S.A., 81 (1984) 2359.
222 C.V. Shank, E.P. Ippen and R. Bersohn, Science, 193 (1976) 50.
223 L.J. Noe, W.G. Eisert and P.M. Rentzepis, Proc. Natl. Acad. Sci. U.S.A., 75 (1978) 573.
224 B.I. Greene, R.M. Hochstrasser, R.B. Weisman and W.A. Eaton, Proc. Natl. Acad. Sci. U.S.A., 75 (1978) 5255.
225 W.A. Saffran and Q.H. Gibson, J. Biol. Chem., 252 (1977) 7955.
226 D.A. Chernoff, R.M. Hochstrasser and A.W. Steele, Proc. Natl. Acad. Sci. U.S.A., 77 (1980) 5606.
227 J.L. Martin, A. Migus, C. Poyart, Y. Lecarpentier, R. Astier and A. Antonetti, Proc. Natl. Acad. Sci. U.S.A., 80 (1983) 173.
228 A.H. Reynolds, S.D. Rand and P.M. Rentzepis, Proc. Natl. Acad. Sci. U.S.A., 78 (1981) 2292.
229 J.A. Hutchinson, T.G. Traylor and L.J. Noe, J. Am. Chem. Soc., 104 (1982) 3221.
230 D.A. Duddell, R.J. Morris, N.J. Mutucumary and J.T. Richards, Photochem. and Photobiol., 31 (1980) 479.
231 J.L. Martin, A. Migus, C. Poyart, Y. Lecarpentier, A. Antonetti and A. Orzag, Biochem. Biophys. Res. Commun., 107 (1982) 803.
232 P.A. Cornelius, A.W. Steele, D.A. Chernoff and R.W. Hochstrasser, Proc. Natl. Acad. Sci. U.S.A., 78 (1981) 7526.
233 P.A. Cornelius, R.M. Hochstrasser and A.W. Steele, J. Mol. Biol., 163 (1983) 119.
234 D.W. Dixon, C. Kirmaier and D. Holten, J. Am. Chem. Soc., 107 (1986) 808.

235 J.O. Alben, D. Beece, S.F. Bowne, W. Doster, L. Eisenstein, H. Frauenfelder, D. Good, J.D. McDonald, M.C. Marden, P.P. Moh, L. Reinisch, A.H. Reynolds, E. Shyamsunder and K.T. Yue, Proc. Natl. Acad. Sci. U.S.A., 79 (1982) 3744.
236 M. Naguno, M. Nicol and M.A. El-Sayed, J. Phys. Chem., 85 (1981) 2435.
237 H. Shimada, T. Iizuka, R. Ueno and Y. Ishimura, FEBS Lett., 98 (1979) 290.
238 M. Hoshimo, S. Arai, M. Yamaji and Y. Hama, J. Phys. Chem., 90 (1986) 2109.
239 F.G. Fiamingio and J.O. Alben, Biochemistry, 24 (1985) 7964.
240 D.A. Case, B.H. Huynh and M. Karplus, J. Am. Chem. Soc., 101 (1979) 4433.
241 A. Waleh and G.H. Loew, J. Am. Chem. Soc., 104 (1982) 2346.
242 A. Waleh and G.H. Loew, J. Am. Chem. Soc., 104 (1982) 2352.
243 A. Waleh and G.H. Loew, J. Am. Chem. Soc., 104 (1982) 3513.
244 M.A. Stanford and B.M. Hoffman, J. Am. Chem. Soc., 103 (1981) 4104.
245 M. Tsubaki, R.B. Srivastava and N.T. Yu, Biochemistry, 21 (1982) 1132.
246 M. Tsubaki and N.T. Yu, Biochemistry, 21 (1982) 1140.
247 M.A. Walters and T.G. Spiro, Biochemistry, 21 (1982) 6989.
248 R.F.W. Bader, Can. J. Chem., 40 (1962) 1164.
249 I.B. Bersuker, B.G. Vekhter and S.S. Stavrov, in 12th Mendeleev Congress on Pure and Applied Chemistry, Abstr., Nauka, Moscow, 1981, p. 388 (in Russian).
250 I.B. Bersuker, S.S. Stavrov and B.G. Vekhter, Chem. Phys., 69 (1982) 165.
251 M.W. Makinen and A.K. Churg, in A.B.P. Lever and H.B. Gray (Eds.), Iron Porphyrins (Part 1), Addison–Wesley, London, 1983, p. 141.
252 B.M. Dzhagarov, Yu.V. Timinskii, V.S. Chirvonyi and G.P. Gurinovich, Dokl. Akad. Nauk SSSR, 247 (1979) 728.
253 V.S. Chirvonyi, B.M. Dzhagarov and Yu.V. Timinskii, Izv. Akad. Nauk SSSR, Ser. Fiz., 44 (1980) 868.
254 V.S. Chirvonyi, B.M. Dzhagarov, Yu.V. Timinskii and G.P. Gurinovich, Chem. Phys. Lett., 70 (1980) 79.
255 D. Huppert, K.D. Straub and P.M. Rentzepis, Proc. Natl. Acad. Sci. U.S.A., 74 (1977) 4139.
256 V.S. Chirvonyi, B.M. Dzhagarov, A.M. Shul'ga and G.P. Gurinovich, Dokl. Akad. Nauk SSSR, 259 (1981) 1256.
257 T. Kitagawa, Y. Kyogoku, T. Iizuka and M.I. Saito, J. Am. Chem. Soc., 98 (1976) 5169.
258 A.P. Baronavski and J.R. McDonald, Chem. Phys. Lett., 45 (1977) 172.
259 M.D. Morse, K.F. Freed and Y.B. Band, J. Chem. Phys., 70 (1979) 3604.
260 M.D. Morse, K.F. Freed and Y.B. Band, J. Chem. Phys., 70 (1979) 3620.
261 Y.B. Band, M.D. Morse and K.F. Freed, Chem. Phys. Lett., 67 (1979) 294.
262 M.D. Morse and K.F. Freed, Chem. Phys. Lett., 74 (1980) 49.
263 Y.B. Band, K.F. Freed and D.J. Kouri, J. Chem. Phys., 74 (1981) 4380.
264 A.K. Churg, R.S. Danziger and M.W. Makinen, in W.S. Caughey (Ed.), Biochemical and Clinical Aspects of Hemoglobin Abnormalities, Academic Press, New York, 1978, p. 323.
265 M.A. Stanford, J.C. Swartz, T.E. Phillips and B.M. Hoffman, J. Am. Chem. Soc., 102 (1980) 4492.
266 G.N. La Mar, D.B. Viscio, D.L. Budd and K. Gersonde, Biochem. Biophys. Res. Commun., 82 (1978) 19.
267 B.M. Dzhagarov, P.N. Dyl'ko and G.P. Gurinovich, Dokl. Akad. Nauk SSSR, 275 (1984) 765.
268 G.P. Gurinovich, A.N. Sevchenko and K.N. Solovyov, Spectroscopy of Chlorophyll and Related Compounds, Nauka i Tekhnika, Minsk, 1968 (in Russian).
269 M. Gouterman, in D. Dolphin (Ed.), The Porphyrins, Vol. 3, Academic Press, New York, 1978, p. 1.

270 M. Gouterman, J. Chem. Phys., 30 (1959) 1139.
271 C. Weiss, H. Kobayashi and M. Gouterman, J. Mol. Spectrosc., 16 (1965) 415.
272 J.E. Zalesskii, V.N. Kotlo, K.N. Solovyov and S.F. Shkirman, Zh. Prikl. Spectrosk., 20 (1974) 1010.
273 R.J. Platenkamp and G.W. Canters, J. Phys. Chem., 85 (1981) 56.
274 R.J. Platenkamp and M. Noort, Mol. Phys., 45 (1982) 97.
275 H.M. van Noort, B. Wirnitzer, J. Schmidt and J.H. van der Waals, Mol. Phys., 45 (1982) 1259.
276 S.S. Stavrov, Teor. Eksp. Khim., 23 (1987) 699.
277 D.J. Robbins, Theor. Chim. Acta, 33 (1974) 51.
278 B.M. Hoffman and M.A. Ratner, Mol. Phys., 35 (1978) 901.
279 R.H. Felton and N.-T. Yu, in D. Dolphin (Ed.), The Porphyrins, Vol. 3, Academic Press, New York, 1978, p. 347.
280 M.H. Perrin, M. Gouterman and C.L. Perrin, J. Chem. Phys., 50 (1969) 4137.
281 J.A. Shelnutt, J. Chem. Phys., 72 (1980) 3948.
282 J.A. Shelnutt, J. Chem. Phys., 74 (1981) 6644.
283 L. Bajema, M. Gouterman and C.B. Rose, J. Mol. Spectrosc., 39 (1971) 421.
284 L. Edwards, M. Gouterman and C.B. Rose, J. Am. Chem. Soc., 98 (1976) 7638.
285 M. Gouterman, Ann. N.Y. Acad. Sci., 206 (1973) 70.
286 G.W. Canters and J.H. van der Waals, in D. Dolphin (Ed.), The Porphyrins, Vol. 3, Academic Press, New York, 1978, p. 531.
287 G.W. Canters, J. Chem. Phys., 74 (1981) 157.
288 R.J. Platenkamp, Mol. Phys., 45 (1982) 113.
289 K.N. Solovyov, I.V. Stanishevskii and A.S. Starukhin, Zh. Prikl. Spectrosk., 40 (1984) 765.
290 J.A. Shelnutt, L.D. Cheung, R.C.C. Chang, N.-T. Yu and R.H. Felton, J. Chem. Phys., 66 (1977) 3387.
291 G.A. Schick and D.F. Bocian, J. Am. Chem. Soc., 106 (1984) 1682.
292 J.H. van der Waals, W.G. van Dorp and T.J. Schaafsma, in D. Dolphin (Ed.), The Porphyrins, Vol. 4, Academic Press, New York, 1979, p. 257.
293 N. van Dijk, M. Noort and J.H. van der Waals, Mol. Phys., 44 (1981) 891.
294 N. van Dijk, M. Noort, S. Voelker, G.W. Canters and J.H. van der Waals, Chem. Phys. Lett., 71 (1980) 415.
295 W.A.J.A. van der Poel, A.M. Nuijs and J.H. van der Waals, J. Phys. Chem., 90 (1986) 1537.
296 J.A. Kooter and J.H. van der Waals, Mol. Phys., 37 (1979) 997.
297 N.-T. Yu and R.B. Srivastava, J. Raman Spectrosc., 9 (1980) 166.
298 P.M. Champion and A.C. Albrecht, J. Chem. Phys., 75 (1981) 3211.
299 B.R. Stallard, P.R. Callis, P.M. Champion and A.C. Albrecht, J. Chem. Phys., 80 (1984) 70.
300 P.M. Champion, Chem. Phys. Lett., 86 (1982) 231.
301 M.Z. Zgiersi and M. Pawlikowski, Chem. Phys. Lett., 57 (1978) 438.
302 W. Siebrand and M.Z. Zgierski, Chem. Phys. Lett., 63 (1979) 226.
303 M.Z. Zgierski and M. Pawlikowski, Chem. Phys., 65 (1982) 335.
304 M.Z. Zgierski, Chem. Phys., 65 (1982) 369.
305 M.Z. Zgierski, Chem. Phys. Lett., 111 (1984) 553.
306 P.M. Callahan and G.T. Babcock, Biochemistry, 20 (1981) 952.
307 R.B.M. Koehorst, J.F. Kleibeuker, T.J. Schaafsma, D.A. de Bie, B. Geurtsen, R.N. Henrie and H.C. van der Plas, J. Chem. Soc., Perkin Trans. 2, (1981) 1005.

308 M.Z. Zgierski, Chem. Phys. Lett., 124 (1986) 53.
309 L.K. Lee, N.H. Sabelli and P.R. Breton, J. Phys. Chem., 86 (1982) 3926.
310 A.M. Shulga, L.L. Gladkov, I.V. Stanishevskii and A.S. Starukhin, Teor. Eksp. Khim., 21 (1985) 431.
311 N.V. Dubinin and A.T. Vartanyan, Opt. Spektrosk., 49 (1980) 1184.
312 A.J. McHugh, M. Gouterman and C. Weiss, Jr., Theor. Chim. Acta, 24 (1972) 346.
313 A.M. Schaffer and M. Gouterman, Theor. Chim. Acta, 25 (1972) 62.
314 S.J. Chantrell, C.A. McAuliffe, R.W. Munn, A.C. Pratt and R.F. Weaver, Bioinorg. Chem., 7 (1977) 283.
315 J.D. Petke, G.M. Maggiora, L.L. Shipman and R.E. Christoffersen, J. Mol. Spectrosc., 71 (1978) 64.
316 S.S. Dvornikov, V.N. Knyukshto, V.A. Kuzmitsky, A.M. Shulga and K.N. Solovyov, J. Lumin., 23 (1981) 373.
317 D.C. Rawlings, E.R. Davidson and M. Gouterman, Theor. Chim. Acta, 61 (1982) 227.
318 M.B. Masthay, L.A. Findsen, B.M. Pierce, D.F. Bocian, L.S. Lindsey and R.R. Birge, J. Chem. Phys., 84 (1986) 3901.
319 W. Gulbinas, B.M. Dzhagarov, W. Kabelka and J. Savitskene, in Laser Spectroscopy of Complex Molecules, Abstr. of Seminar Dedicated to R.A. Avarmaa, Acad. Sci. of ESSR, Tallin, 1988, p. 34.